



# **Neuromeric organization of the midbrain-hindbrain boundary region in zebrafish**

DISSERTATION

zur Erlangung des akademischen Grades

**Doctor rerum naturalium  
(Dr. rer. nat.)**

vorgelegt

der Fakultät Mathematik und Naturwissenschaften

der Technischen Universität Dresden

von

**Dipl.-Biol. Tobias Langenberg**

geboren am 21.08.1974 in Hann. Münden

Gutachter: Prof. Dr. Michael Brand  
Prof. Dr. Herwig O. Gutzeit  
Prof. Dr. Stephen Wilson

Eingereicht am: 01.10.2004  
Tag der Verteidigung:



Can I have some remedy?  
Remedy for me please  
Cause if I had some remedy  
I'd take enough to please me

("Remedy" The Black Crowes)

Saturday I'm running wild  
And all the lights are changing red to green  
Moving through the crowd I'm pushing  
Chemicals all rushing through my bloodstream

Sunday all the lights of London  
Shining , Sky is fading red to blue  
I'm kicking through the Autumn leaves  
And wondering where it is I might be going to

("Babylon", David Gray)

# Acknowledgements

For continuous support and for being a positive driving force, I am grateful to Michael Brand.

I thank past, present and one returned member of the Brand lab, as well as members of the Heisenberg and Oates lab, for creating a very good working atmosphere, for feedback, stimulating discussions and for the cheerful noise that filled the empty new labs at the MPI.

For listening, I especially thank Chris, Carl-Philip, Alexander and Irinka.

I wish to thank the members of my thesis advisory committee for their time and feedback: Prof. H. O. Gutzeit and Carl-Philip Heisenberg.

For reviewing my thesis, I am grateful to Prof. Gutzeit and Prof. Stephen Wilson.

Special thanks to Arndt (the negative feedback inhibitor) for reading and correcting this thesis.

For being a light in very dark times and so much more, I thank Janina.



# Summary

The neuromeric concept of brain formation has become a well-established model to explain how order is created in the developing vertebrate central nervous system. Neuromeres are evolutionary conserved units of gene expression, differentiation and are compartmentalized on the cellular level: Each neuromere comprises a lineage-restricted population of cells that does not intermingle with cells from neighboring compartments.

The units of the vertebrate hindbrain, the rhombomeres, serve as the best-studied examples of neuromeres. Here, the lineage restriction mechanism has been found to function on the basis of differentially expressed adhesion molecules. To date, evidence for the existence of neuromeres in more anterior parts of the brain, based on lineage restriction analyses, is still scarce.

The focus of this study is the midbrain-hindbrain boundary (mhb) region, where the juxtaposition of the mesencephalon and metencephalon gives rise to a signaling center, termed the midbrain-hindbrain or isthmic organizer. Evidence for lineage restriction boundaries in the mhb region is still controversial, with some very recent studies suggesting the existence of a lineage boundary between the mesencephalon and metencephalon and others rejecting this. As none of these studies analyzed cell behavior with cellular resolution, the controversies could not be resolved.

Here, I present data strongly supporting the existence of a compartment boundary between the posterior midbrain and anterior hindbrain territory. I base this proposition on cell-tracing experiments with single cell resolution. By connecting the traces to a molecular midbrain marker, I establish a link between cellular behavior and molecular identity.

In the second part, I present a novel tissue explant method for the zebrafish that has the potential to serve numerous developmental studies, especially imaging of so far inaccessible regions of the embryo.

# Table of Contents

<b><u>NEUROMERIC ORGANIZATION OF THE MIDBRAIN-HINDBRAIN BOUNDARY REGION IN ZEBRAFISH</u></b>	<b>2</b>
<b><u>ACKNOWLEDGEMENTS</u></b>	<b>5</b>
<b><u>SUMMARY</u></b>	<b>7</b>
<b><u>TABLE OF CONTENTS</u></b>	<b>8</b>
<b><u>ABBREVIATIONS</u></b>	<b>10</b>
<b><u>MATERIALS AND METHODS</u></b>	<b>11</b>
EMBRYO MEDIA, SOLUTIONS, CHEMICALS AND MATERIALS	11
FISH MAINTENANCE	13
PLASMID DNA	13
<i>IN-SITU</i> HYBRIDIZATION	14
ANTI-OTX ANTIBODY STAINING	15
RNA INJECTION	16
CELL TRANSPLANTATION	17
DIJ LABELING	17
IONTOPHORETIC SINGLE CELL INJECTION	17
IMAGE ACQUISITION AND PROCESSING	19
NUCLEI TRACKING AND PLOTTING	20
<b>METHODS USED IN THE EMBRYONIC EXPLANT PART</b>	<b>23</b>
CULTURE MEDIA PREPARATION	23
PREPARATION OF VITAL STAINS	23
INJECTION SOLUTION	23
PREPARATION OF TUNGSTEN NEEDLES AND EYELASH TOOLS	23
AGAROSE IMMOBILIZATION OF WHOLE EMBRYOS	24
REMOVAL OF YOLK CELL	24
PLASMA CLOT PREPARATION	25
EXPLANT PREPARATION AND MOUNTING	25
<b><u>INTRODUCTION</u></b>	<b>27</b>
ZEBRAFISH NEURULATION	27
NEURAL INDUCTION AND INITIAL NEURAL PATTERNING	28
SECONDARY NEUROEPITHELIAL ORGANIZERS	29
THE NEUROMERIC MODEL OF BRAIN REGIONALIZATION	30
A MODERN DEFINITION OF NEUROMERES	31
THE RHOMBENCEPHALON	32
LINEAGE RESTRICTION MECHANISMS	33
MORE COMPARTMENTS IN THE VERTEBRATE BRAIN?	36
SPECIALIZED BOUNDARY CELLS	36
LINEAGE RESTRICTION AND ORGANIZERS	37



<b>EMBRYONIC EXPLANTS</b>	<b>39</b>
<b>AIM OF THE THESIS</b>	<b>41</b>
I: IS THE MIDBRAIN-HINDBRAIN BOUNDARY IN ZEBRAFISH A LINEAGE RESTRICTION BOUNDARY?	41
II: WHAT IS THE MECHANISM BEHIND THE OBSERVED LINEAGE RESTRICTION?	41
III: ARE THERE MORE COMPARTMENT BOUNDARIES IN THE MHB AREA?	41
<b>RESULTS</b>	<b>42</b>
<b>LINEAGE RESTRICTION AT THE MIDBRAIN-HINDBRAIN BOUNDARY</b>	<b>42</b>
MORPHOLOGICAL CHANGES DURING MIDBRAIN-HINDBRAIN BOUNDARY FORMATION	42
BEHAVIOR OF INDIVIDUAL CELLS	45
LINEAGE LABEL BY DII APPLICATION	47
SINGLE CELL LINEAGE ANALYSIS BY IONTOPHORETIC INJECTION	47
CLONE SIZE AND CLONAL SPREAD AFTER SINGLE CELL INJECTIONS	49
IMAGING OF INDIVIDUAL NUCLEI	50
THE MHB IS A LINEAGE RESTRICTION BOUNDARY	53
LINEAGE RESTRICTION BOUNDARY AND MORPHOLOGICAL BOUNDARY DO NOT MATCH	59
<b>CANDIDATE GENES FOR THE LINEAGE RESTRICTION MECHANISM</b>	<b>60</b>
<b>EMBRYONIC EXPLANTS</b>	<b>63</b>
AMP-PNP BLOCKS CURLING OF EXPLANTS	63
MOTIONAL STABILITY OF IMMOBILIZED EXPLANTS	64
NORMAL MORPHOGENESIS IN CULTURED EXPLANTS	64
APOPTOTIC CELL DEATH IS NOT ELEVATED IN CULTURED EXPLANTS	66
GENE EXPRESSION IN EXPLANTED HEAD RUDIMENTS	66
CROSS-SECTIONAL AND VENTRAL IMAGING OF EMBRYONIC EXPLANTS	68
<b>DISCUSSION</b>	<b>69</b>
<b>LINEAGE RESTRICTION AT THE MIDBRAIN-HINDBRAIN BOUNDARY</b>	<b>69</b>
<b>EMBRYONIC EXPLANTS</b>	<b>75</b>
<b>MOVIE DESCRIPTIONS</b>	<b>78</b>
<b>REFERENCES</b>	<b>80</b>
<b>APPENDIX</b>	<b>90</b>
ISTHMUS TO MIDBRAIN TRANSFORMATION IN <i>ACE</i>	90

# Abbreviations

SI units and symbols of standard multiples (m,  $\mu$ , etc.) are not listed. Additional abbreviations are introduced and explained in the text.

AMP-PNP	Adenosine 5' ( $\beta$ , $\gamma$ -imido) triphosphate,
ANR	anterior neural ridge
AP	alkaline phosphatase
a-p	anterior-posterior
DIC	differential interference contrast
DIG	digoxigenin
DMSO	dimethylsulfoxide
DNA	deoxyribonucleic acid
EDTA	ethylene di-amine tetra-acetate
GFP	green fluorescent protein
hpf	hours post fertilization
Hyb	hybridization buffer
ISH	<i>in-situ</i> hybridization
MAB(T)	maleic acid buffer (+ Tween)
mhb	midbrain-hindbrain boundary
o/n	over night
PE	polyethylene
PBS(T)	phosphate buffered saline (+Tween)
PFA	paraformaldehyde
RNA	ribonucleic acid
rpm	rounds per minute
RT	room temperature
ss	somites
SSC(T)	sodiumchloride/sodiumcitrate buffer (+Tween)
TRITC	trimethyl rhodamine isothiocyanate
ZLI	zona limitans intrathalamica

# Materials and Methods

## Embryo media, solutions, chemicals and materials

AMP-PNP	Calbiochem 120002
anti-DIG antibody	Roche 1093274
anti-fluorescein antibody	Roche 1426338
anti-Otx antibody	gift from Antonio Simeone
anti-rabbit, goat, TRITC coupled	Jackson Immuno Research (dianova GmbH) 111-025-144
BM Purple	Roche 1442074
BODIPY 505/515 (unconjugated)	Molecular Probes / Invitrogen D3921
BODIPY-Ceramide	Molecular Probes / Invitrogen D-3521 BODIPY FL C <sub>5</sub> – Ceramide
bovine plasma	Sigma P-4639
capillaries (injection, iontophoresis)	WPI 100F-3 borosilicate capillaries, outer diameter 1.0 mm, inner diameter 0.75 mm (with filament)
capillaries (transplantation)	WPI 100-3 (without filament)
Danieau's embryo medium	58 mM NaCl, 0.7 mM KCl, 0.4 mM MgSO <sub>4</sub> x 7 H <sub>2</sub> O, 0.6 mM Ca(NO <sub>3</sub> ) <sub>2</sub> x 4 H <sub>2</sub> O, 5 mM HEPES, pH 7.2, 1x penicillin-streptomycin
DIG block	2% blocking reagent (Roche 1096176) dissolved in MABT
Dil (1,1'-dioctadecyl-3,3,3',3'-tetramethylindocarbocyanine perchlorate, DiI <sub>C18</sub> (3))	Molecular Probes/Invitrogen D-282
E3 embryo medium	5 mM NaCl, 0.17 mM KCl, 0.33 mM CaCl <sub>2</sub> x 2 H <sub>2</sub> O, 0.33 mM MgSO <sub>4</sub> x 7 H <sub>2</sub> O, 10 <sup>-5</sup> % Methyleneblue
FastRed substrate	Roche 1496549
glass rings	Fisher Scientific MNK-145-030K
Hyb <sup>-</sup>	50% deionized formamid; 5x SSC pH 6.0; 0.1% Tween-20
Hyb <sup>+</sup>	Hyb <sup>-</sup> + 0.5 mg/ml torula (yeast) RNA; 50 µg/ml heparin
Leibovitz L-15 medium	Invitrogen 21083-027
LMP agarose	Invitrogen 15517-014

MABT	100 mM maleic acid; 150 mM NaCl adjusted to pH 7.5 with NaOH, 0.1% Tween-20
NGS (normal goat serum)	Invitrogen 16210-072
penicillin-streptomycin	Sigma P 0781: 10000 U penicillin, 10 mg/ml streptomycin
penicillin/streptomycin/antimycotic	Invitrogen 15240-096
1x PBS	1,7 mM $\text{KH}_2\text{PO}_4$ , 5,2 mM $\text{Na}_2\text{HPO}_4$ , 150 mM NaCl
PBST	1x PBS + 0.1% Tween 20
PBT	PBST + 0.8% Triton-X100
PFA	4% paraformaldehyde in 100 mM phosphate buffer, pH 7.4
proteinase K	Sigma P 6556
rhodamine dextrane (“mini-ruby”)	Molecular Probes/Invitrogen, D-3312
20x SSC	for 1 liter: 175.3 g NaCl; 88.2 g Na-citrate (x2 $\text{H}_2\text{O}$ ), pH adjusted to 6.0 with 1 M citric acid
SSCT	SSC + 0.1% Tween-20
silicone grease	Beckman 335148
syringe needle (long)	WPI MF34G-5
thrombin	Sigma T-4648
torula RNA	Sigma R 6625
trypsin	Sigma T 7409
tungsten wire	Clark Electromedical Instruments TW10-3 and WPI TGW1510

## Fish maintenance

Zebrafish were raised and kept under standard laboratory conditions at 28.0°C (Westerfield, 1994; Brand and Granato, 2000). To delay development, I incubated embryos at 18°C from the shield stage onwards or at RT directly after fertilization. Transgenic fish for the histone H2A.F/Z:GFP fusion line were obtained from the Campos-Ortega lab (Pauls et al., 2001).

## Plasmid DNA

Plasmid DNA was transformed into bacteria, isolated and purified according to standard protocols.

### Plasmid list

The list includes all plasmids that I received from various labs. More detailed information is given in the Brand lab's plasmid database.

<b>plasmid</b>	<b>vector</b>	<b>information</b>	<b>database #</b>
Eph B4b	pCS2+	full length	353
Eph B4b DN	pCS2+	dominant negative construct	354
ephrin A1	pBUT2	full length	351
ephrin A1 – GPI	pBUT2	without GPI linker, soluble	352
EphB4a	pCS2+	full length	364
ephrin B1	pBK-CMV	full length	373
ephrin B2b	pBK-CMV	full length	374
ephrin B3	pBK-CMV	full length	375
ephrin B2b – GPI	pCS2+	without GPI linker, soluble	376
ephrin B2a	pBUT2	full length	559
ephrin B2a	pBK-CMV	full length	567
ten-m3	pBSK+	tenascin homolog	373
ten-m4	pBSK+	tenascin homolog	374

## *In-situ* hybridization

### Probe preparation

*In-situ* hybridization was essentially carried out as described by Reifers et al. (Reifers et al., 1998). Approximately 10 µg of plasmid DNA were digested with the appropriate restriction enzyme to produce a linearized template with 3 µl restriction enzyme in a final volume of 100 µl for 2 hours at 37°C. After purification by phenol/chloroform extraction and ethanol precipitation, the DNA was dissolved in 20 µl sterile water and 1 µl was checked for concentration on an agarose gel. 1 µg of this template DNA was mixed with 2 µl NTP mix, 2 µl or 4 µl transcription buffer (10x or 5x, respectively) and 1 µl RNase inhibitor, the volume was adjusted to 18 µl with sterile water and the reaction started by adding 2 µl of the appropriate RNA polymerase. After 2 h incubation at 37°C, 2 µl 0.2 M EDTA pH 8.0, 2.5 µl 4 M LiCl and 75 µl ice-cold 100% ethanol were added, vortexed quickly and incubated for at least 30 min at –80°C (or o/n at –20°C) to precipitate the RNA. RNA was then pelleted by 30 min centrifugation at 13000 rpm at 4°C in a standard benchtop centrifuge.

I used probes for the following genes: *otx2* (Mori et al., 1994), *gbx2* (Rhinn et al., 2003), *wnt1* (Kelly et al., 1993), *fgf8* (Reifers et al., 1998), *EphB4a/b* (Durbin et al., 1998; Cooke et al., 2001), *ephrinB2a/b* (Chan et al., 2001), *ephrinA5a/b* (Brennan et al., 1997), *EphA4b* (Xu et al., 1994)

### α-DIG-AP preabsorption

Antibody preabsorption reduces unspecific staining. 50-100 fixed embryos of various stages were minced with a small pestle and incubated with 1 ml of MABT and 5 µl α-DIG-AP on a shaker o/n at 4°C. Then, embryos were spun down by centrifugation at max. speed for 2 min and 1 ml of the supernatant was recovered. The centrifugation can be repeated to enhance recovery of the antibody, which was then diluted to a final concentration of 1:4000 in MABT + 2% DIG-block. Antibody was reused and stored in the presence of 0.01% sodium azide at 4°C for several months or until signal intensity dropped.

### Hybridization

Dechorionated embryos were fixed for at least 4 h at RT or o/n at 4°C in 4% PFA, washed in PBST and transferred for at least 30 min to 100% methanol (can be stored for months at –20°C), rehydrated with PBST at RT and washed in PBST. After long storage, embryos should be refixed for 30 min with 4% PFA at RT and washed with PBST. For permeabilisation, embryos were then

digested with proteinase K (final concentration: 10 µg/ml in PBST) for 1 to 8 min at RT (depending on the developmental stage of the embryos), washed quickly once with PBST and refixed in 4% PFA for 30 min at RT. Embryos were then rinsed and washed in PBST at RT and transferred into prewarmed Hyb<sup>+</sup> solution for at least 1 h at 68°C on a shaker (all subsequent steps on a shaker at 68°C). Hyb<sup>+</sup> was replaced with the prewarmed RNA-probe in Hyb<sup>+</sup>, and embryos were incubated o/n. The probe was taken off (can be stored at -20°C and reused several times), embryos were washed 1x 5 min in Hyb<sup>-</sup>, 3x 10 min in 25% Hyb<sup>-</sup> in 2x SSCT, once 5 min in 2x SSCT and 2x 30 min in 0.2x SSCT. (All subsequent steps on a shaker at RT). Then, embryos were washed once 5 min in 50% 0.2x SSCT / 50% MABT and once 5 min in MABT, blocked for 1 h in MABT + 2% DIG block and incubated for at least 2 h at RT (or o/n at 4°C) in α-DIG-AP (preabsorbed; 1:4000 dilution in MABT + 2% DIG block). After removal of α-DIG-AP, embryos were once rinsed and then washed 4x for 15 min at RT in MABT and transferred into 24- or 48-well plates for detection with BM Purple substrate. I stopped the reaction by repeated washing in PBST and subsequent fixation for at least 30 min with 4% PFA at RT. For photography, embryos were washed with PBST and cleared in 70% glycerol in PBS.

For double ISH, embryos were hybridized with a probe mix (DIG-labeled and fluorescein-labeled RNA-probes) and processed as described above. After BM Purple detection, embryos were washed in PBST, refixed in 4% PFA for 30 min at RT and washed in PBST. To inactivate alkaline phosphatase, embryos were treated with 0.1 M glycine / HCl, pH 2.2 for 3x 5 min and washed 4x 5 min with PBST. Embryos were then washed once 5 min in MABT, blocked for 1 h in MABT + 2% DIG block and incubated o/n at 4°C in freshly diluted α-fluorescein-AP (1:1000 dilution in MABT + 2% DIG block). After removal of α-fluorescein-AP (cannot be reused), embryos were rinsed and then washed 4x 15 min at RT in MABT, once 5 min in 0.1 M Tris/HCl pH 8.2 and transferred into 24- or 48-well plates for detection with freshly prepared FastRed substrate in 0.1 M Tris/HCl pH 8.2. Stainings were developed to the desired intensity in the dark and subsequently treated as described above.

## Anti-Otx antibody staining

Embryos were fixed in 4% PFA o/n at 4°C, washed with 1x PBST, washed once 5 min with distilled water and moved to 100% methanol at -20°C for at least 30 min. After transfer to PBT and washing, embryos were digested with 0.0025% Trypsin in PBT on ice (5 min for embryos between 20 and 24 hpf). Trypsin was removed and embryos postfixed for 30 min with 4% PFA at RT,

washed in PBT and blocked for 1-2 h in NGS-PBT (PBT + 10% heat inactivated Normal Goat Serum (NGS), 1% DMSO). Antibody incubations were as follows: Primary antibody (rabbit polyclonal directed against *Drosophila* orthodenticle) o/n 1:3000 in PBT with 1% NGS (without DMSO, antibody can be reused, add 0.01% Na-Azide). Embryos were washed for at least 1 h in PBT with several changes. Secondary antibody 1:200 (Jackson Immuno Research TRITC coupled) in PBT for 2 h at RT or o/n at 4°C. Embryos were washed for at least 1 h, postfixed for 30 min in 4% PFA at RT, washed again and moved to 70% glycerol.

## RNA injection

### Embryo preparation

For injection experiments, I harvested embryos from crosses into petridishes at the 1-cell stage in E3 medium directly after spawning. To mount the embryos for injection, I aligned them along the edge of a slide positioned in an 85 mm petridish lid. Excess medium was sucked off so that capillary force made the embryos adhere to the edge of the slide. RNA was then injected through the chorion.

### Injection capillaries

Thin wall borosilicate glass capillaries with an internal filament were used, which allows backfilling. Capillaries were pulled with a Flaming/Brown puller (Sutter Instruments P-97) to the desired shape and tip diameter. Before filling, I broke off capillary tips.

### Injection

All injections were done with a pneumatic pico pump (WPI), mechanical micromanipulators (Narishige), and standard capillary holders (WPI). To determine the injection volume, the diameter of a droplet injected into mineral oil was measured. The injection volume was then adjusted by changing the pulse duration and/or strength. Typically, 1-2 nl were injected. For cytoplasmic GFP injection, about 100 pg of GFP RNA was injected.



## Cell transplantation

For transplantation, donor embryos were fluorescently labeled by injection of cytoplasmic GFP RNA and used for grafts at shield stage.

Transplantations were performed in Danieau's medium using thin wall borosilicate glass capillaries without an internal filament in agarose-coated petridishes, using an air-filled assembly consisting of a capillary, the capillary holder and manipulator, attached to PE-tubing and a 1 ml syringe to control the graft. Single cells or groups of cells were sucked from the donor and expelled into the host.

## Dil labeling

To coat labeling capillaries (thin-wall borosilicate as used for injections), Dil was diluted to 0.5 mg/ml in 100% ethanol, a small drop spread out on a slide and carefully heated up to max. 70°C. Capillaries were then moved through the molten Dil, which sticks to their outer surface. Embryos were dechorionated manually and mounted in 1.5% low melting point agarose in Danieau's medium (see 2-photon confocal microscopy). To prevent drying-out, a few drops of Danieau's medium were pipetted onto the agarose. A window was then cut into the agarose to allow access to the embryo. Using a capillary holder and micromanipulator setup, the coated capillary was pushed through the embryo's epidermis and inserted into the neuroepithelium for at most 10 seconds. I controlled label intensity by standard fluorescent microscopy directly after labeling. Each capillary was reused until the Dil coat came off.

## Iontophoretic single cell injection

### Capillary preparation

High-resistance capillaries are the key to successful iontophoretic injection. Thin-walled borosilicate capillaries (WPI) were pulled on a box filament puller (Sutter Instruments P97) such that the tip was just open. To evaluate tip size, capillaries were placed under a 40x dry objective. A blue shining tip is characteristic for high-resistance capillaries. Capillary resistance can be measured by applying holding current and monitoring the mV potential output of the amplifier. Good capillaries will have a resistance of >35 MΩ when filled with 0.2 M KCl

### Injection setup

To facilitate injection, a stage-mounted micromanipulator was used. The microscope has to be placed onto an air-table to minimize vibrations. The electric circuit comprises the capillary, an electrochemical Ag/AgCl half-cell holding the capillary, the amplifier's headstage and the second reference Ag/AgCl electrode placed into the medium. It is very important to ground the amplifier. The amplifier is used to set the potential between the two electrodes to zero (by adjusting offset), such that no dye flows out of the capillary (monitor using life fluorescence) without applied holding current. It is very important to ground the amplifier, otherwise stray potentials will cause dye to leak from the capillary. Low-resistance capillaries will leak dye at this point and have to be discarded.

### Injection

Capillaries were backfilled with 1  $\mu$ l 3% rhodamine dextrane ("mini ruby") and placed in a moist chamber for several hours. Directly before use, capillaries were carefully backfilled with 0.2 M KCl using a long syringe needle. Embryos were manually dechorionated in 1x Danieau's medium on 1.5 - 2% agarose and placed in agarose wells (Westerfield, 1994) in an 85 mm petridish lid. Under low magnification and brightfield illumination, I approximated the capillary to the embryo. The injection was carried out using a 40x dipping objective. The capillary tip was moved into contact with the target cell (vibration-free, using the external drive of the manipulator) and forced through the cell's membrane by "ringing" ("buzzer" on some amplifiers) the capacitance. Sometimes this was already sufficient to fill the target cell. Labeling intensity was controlled under direct fluorescent illumination using standard TRITC/Rhodamine filter sets. Application of 0.5 to 5 nA holding current slowly filled the cell with the dye. Switching on the holding current was sometimes sufficient to penetrate the target cell's membrane, in which case capacitance ringing was not necessary. To avoid damage to the cell, the capillary tip was retracted quickly once the cell was brightly labeled. Under 40x epifluorescence, the quality of the label and the number of injected cells were checked. For reference see (Fraser, 1996).

## Image acquisition and processing

### Standard confocal microscopy

*In-situ* stained embryos were imaged on a Zeiss LSM 510 confocal microscope with a 40x oil immersion objective. Anti-Otx stained embryos were imaged using a 60x water immersion objective on the same microscope. Images were exported as tiff-format series using the LSM Image Reader software (Zeiss) and processed in Adobe Photoshop.

### 2-photon confocal microscopy

Live embryos were mounted in 1.5% low melting point agarose in Danieau's medium in a small self-assembled imaging chamber (Concha and Adams, 1998) comprising a glass ring, glued with silicon-grease between a coverslip and a slide. The embryos were pipetted into the warm agarose (39°C) and transferred into the ring on the coverslip with a sufficient amount of agarose. Embryos were oriented and mounted as close to the coverslip as possible with thin and blunt tungsten wire tools. Once the agarose had gelled, the ring was filled with medium and the slide placed on top. This chamber can be used for inverted and upright microscopy.

For time lapse microscopy, stacks of 40-50 images with a z-spacing of 1.5  $\mu\text{m}$  and a time interval of 3-4 min were acquired over 8-12 h using a BioRad inverted confocal system with a 60x Nikon water immersion objective. The infrared laser was adjusted to an intensity that gave a good signal quality in the middle portion of the stacks, using high gain, which assured that nuclei were not harmed by long-term imaging. No absolute value for laser intensities can be given, as variabilities in laser output are in the nature of the 2-photon system, but the output was usually set to about 40% of maximum.

BioRad Image stacks were opened using ImageJ with the BioRad reader drop-in, exported as tiff-series, renamed with File Buddy (ScyTag Software) and imported into the NIHImage4D version (R. Adams).

Alternatively, image stacks were assembled into 4D-stacks using the Metamorph (Visitron Systems GmbH) multi-dimensional data review drop-in.

### Spinning disc confocal microscopy

Embryos were mounted as described above. I acquired z-stacks every 10 min over 20-30 h with a 25x multi-immersion objective. Due to the fixed pinhole size of the spinning disc, z-resolution was limited to about 5  $\mu\text{m}$ . Stacks were exported to tiff-format single files and analyzed in NIH image with a macro written by K. Anderson.

## Nuclei tracking and plotting

Nuclei were manually tracked in 4D stacks assembled in NIHImage4D (see above); coordinates (xy-center and z-plane) were put into Excel files. The following notation scheme was used:

cell name	Otx code	start row	end row	division	coordinate triplets
1, 1b, 1c etc	0 or 1	(1 to 5)	(1 to 25)	in tp	x, y in pixels z in planes

*cell name*: Cells (nuclei) are numbered with running numbers, starting from 1. Daughter cells are named using the main number followed by “b”, “c” and so forth.

*Otx code*: Can be 0 or 1, whether or not the nucleus is positive for anti-Otx antibody staining at the end of the time lapse.

*start row*: Nucleus position in rows distance from the common boundary of Otx-positive and Otx-negative nuclei at the start of the time lapse.

*end row*: The same as start row, this time at the end of the time lapse.

*division*: Time of birth of a daughter cell in time points (tp).

*coordinate triplets*: Coordinates for the nucleus’ xyz center in pixels (xy) and plane (z). Triplets are noted at about every hour of the time lapse (corresponding to about every 25 time points) and/or at critical positions (directly before microscope stage-shifts or z-shifts).

Coordinates were processed with self-written files in Matlab (The Mathworks GmbH). Generalized codes for 3D-plots (“scatter3” base function) and arrow plots (“plot” base function) are given below. The code is annotated with remarks following the “%” sign (Matlab notation), code is bold.

### Scatter3 plot

```
% clears workspace and command window
clc
clear
% sets marker area in points squared for the outline (s2) and the filled marker (s1)
s=130;
s2=150;
% reads Excel source file into variable source
source=xlsread("sourcefile name here");
% the second column of "source" is used for the otx code assignment
otxstate=source(:,2);
% reads the length of column 2 into rowsize1
[rowsize1,rowsize]=size(otxstate);
% creates variable r of length rowsize1 with each row entry = 0.5
r=ones(rowsize1,1)*.5;
% creates variable with row entries depending on the otx state and r (0.4 or 0.9)
cvalue=(r.*otxstate) + 0.4;
```

```

% the color matrix is assembled using the same value for each color component
(R,G,B),% thereby creating grey or dark grey values
color=[cvalue, cvalue, cvalue];
% similar to r, with each row value = 0.0
r2=zeros(rowsize1,1);
% creates a color matrix of the same length as color with all entries = 0 (black)
color2=[r2,r2,r2];
% creates a variable for reversing the z position
fullz=ones(rowsize1,1)*50;
% example plot using the subplot function
% opens a new figure window
figure
% opens a 2x2 subplot window with the first subplot in the upper left quadrant
subplot (2,2,1);
% all following plot commands are added into the same plot until "hold off"
hold on;
% plots the inner filled marker using the columns 30 (x), 31 (y) and 32 (z) as
examples,
% calibrated by pixels-to-microns (*0.4 for xy and *1.5 for z) and reverses the z-
values
scatter3( source(:,30)*0.4, source(:,31)*0.4, (fullz-source(:,32))*1.5, s, color,
'filled');
% plots the black ring around each filled marker
scatter3( source(:,30)*0.4, source(:,31)*0.4, (fullz-source(:,32))*1.5, s2 ,color2);
hold off;
% lateral view mode is used
view ([-90 0]);
% dorsal view mode is commented (not used)
% view ([360 90]);
xlabel('x'); ylabel('y'); zlabel('z');

```

### Arrow plot

```

% clears workspace and command window
clc
clear
% reads Excel source file into variable source
source=xlsread('sourcefile name here');
% reads length of the second column of source into matsize
matsize=length(source(:,2));
% converts 0/1 otxcode to -1/1 code for all cells
for i=1:matsize;
    if source(i,2)==1;
        source(i,2)=-1;
    end
end
for i=1:matsize;
    if source(i,2)==0;
        source(i,2)=1;
    end

```

```

    end
end
% sorts source after the second column (otx code)
[y, index]=sort(source(:,2));
sources=source(index,:);
% reads the number of cells with otx code = -1 into getl
getl=length(find(sources(:,2)==-1));
% copies all data of otx negative cells into otxn
otxn=sources(1:getl,:);
% copies all data of otx positive cells into otxp
otxp=sources(getl+1:matsize,:);
% otx positive cells are numbered from 1 to "length of otxp"
xp=(1:length(otxp(:,2)))';
% otx positive start row is stored in ystartp
ystartp=otxp(:,3);
% otx positive end row is stored in yendp
yendp=otxp(:,4);
% otx negative cells are numbered from 1 to "length of otxn"
xn=(1:length(otxn(:,2)))';
% otx negative start row is stored in ystartn
ystartn=otxn(:,3).*otxn(:,2);
% otx negative end row is stored in yendn
yendn=(otxn(:,4)*-1);
%plots otx positive cells
for ix = 1:length(otxp(:,2)),
%plots lines for all cells
    plot([xp(ix) xp(ix)], [ystartp(ix) yendp(ix)],'k-', 'LineWidth',1);hold on
% if startrow > endrow
    if ystartp(ix) > yendp(ix);
%plots arrowheads for backward moving cells
        plot([xp(ix)], [yendp(ix)],'kv', 'MarkerFaceColor',[0.85 0 0]);hold on
% if startrow = endrow
        elseif ystartp(ix)==yendp(ix)
%plots stars for non-movers
            plot([xp(ix)], [yendp(ix)],'r*');hold on
% plots arrowheads for remaining cells ("forward-movers")
            else plot([xp(ix)], [yendp(ix)],'k^', 'MarkerFaceColor',[0.85 0 0]);hold on
        end
    end
end
% plot otx negative cells
for ix = 1:length(otxn(:,2)),
    plot([xn(ix) xn(ix)], [ystartn(ix) yendn(ix)],'k-');hold on
    if ystartn(ix) > yendn(ix);
        plot([xn(ix)], [yendn(ix)],'bv', 'MarkerFaceColor',[0 0 0.85]);hold on
    elseif ystartn(ix)==yendn(ix)
        plot([xn(ix)], [yendn(ix)],'b*');hold on
    else plot([xn(ix)], [yendn(ix)],'b^', 'MarkerFaceColor',[0 0 0.85]);hold on
    end
end
end
hold off

```

## Methods used in the embryonic explant part

### Culture media preparation

A penicillin/streptomycin/antimycotic mixture was added to L-15 amphibian culture medium to a final activity of 100 U/ml for the Penicillin. 67% strength L-15 in sterile water has been shown to be isotonic to zebrafish cells (Peppelenbosch et al., 1995) and is recommended. Some of the experiments were performed in full-strength L-15.

### Preparation of vital stains

Embryos were vitally stained with the fluorescent dye Bodipy 505/515 using the procedures outlined by Cooper (Cooper et al., 1999).

### Injection solution

AMP-PNP was diluted to a final concentration of 40 mM in Millipore water. Owing to its chemical lability, AMP-PNP should be quickly partitioned and frozen at -20°C. 2 µl of the AMP-PNP solution were backfilled into micropipettes. Typically, an 8 nl bolus of the 40 mM AMP-PNP solution was injected into the yolk cell.

### Preparation of tungsten needles and eyelash tools

Tungsten needles were electrolytically sharpened in 5 M NaOH. Briefly, a 20-gauge syringe needle was fastened to the end of a 1 cm<sup>3</sup> tuberculin syringe. The tip of the needle was then cut off using wire cutters. The end of the needle was reopened with needle nose pliers. A tungsten wire was inserted into the syringe opening. The needle was then crimped to hold the wire in place. An alligator electrical connector was attached to the base of the needle, and the needle electrolytically sharpened using about 10 V direct current. Eyelash and hairloop micropositioning tools were prepared according to the procedures of Grinblat (Grinblat, 1999).

## Agarose immobilization of whole embryos

To immobilize whole embryos, it is very convenient to use normal agarose at 0.4 – 0.5%, kept in a water bath or heating block at 42°C. The embryo was pipetted into the agarose, quickly taken out with some molten agarose and poured onto a mounting device for imaging. I recommend the imaging chamber described above (Concha and Adams, 1998). The embryo has to be oriented quickly with an eyelash poker (or equivalent), since the agarose will gel within 10 - 20 seconds, firmly holding the embryo in place.

For long-term time-lapse imaging, a hole for the body axis to elongate was cut into the agarose. This hole allowed the body to extend normally, while maintaining immobilization of the head. The hole was cut using tungsten needles. Embryos survived in agarose without medium exchange for at least 24 h. Low melting point (LMP) agarose is preferable for very young embryos (up to the tailbud stage, 10 hpf), since it can be added at lower temperatures (down to 39°C). This way, yolk cell rupture is less likely to occur. LMP agarose takes much longer to gel than regular agarose, and should be used at higher concentrations (e.g. 0.75 – 1.5%).

## Removal of yolk cell

To retard yolk cell contractility in response to wounding, a non-hydrolysable analog of ATP (AMP-PNP) was microinjected into the yolk cell prior to dissection of the embryo. To efficiently block curling, injection of an 8 nl bolus of 40 mM AMP-PNP was sufficient. Within one minute after injection, the yolk cell's cortex becomes paralyzed. AMP-PNP is membrane impermeable, and thus will not leave the yolk cell and enter the blastoderm. Once the yolk cell's actomyosin networks had been paralyzed, much of the yolk mass within the yolk cell was extruded by gentle pressure applied from a blunt metal microneedle. After the yolk had been extruded, the ventral epidermis covering the yolk cell was split open along the anterior-posterior axis using a tungsten needle, and most of the yolk cell's enveloping layer and underlying epidermis was cut away.



## Plasma clot preparation

To mount explanted pieces of embryonic tissue, I modified the plasma clot technique developed by Gähwiler (Gähwiler, 1981; Gähwiler, 1984a; Gähwiler, 1984b). Lyophilized bovine plasma was first reconstituted in Millipore water, partitioned, and frozen at  $-20^{\circ}\text{C}$ . Thrombin was diluted to 100 U/ml stock concentration, partitioned and frozen at  $-20^{\circ}\text{C}$ . A drop ( $\sim 20\ \mu\text{l}$ ) of reconstituted bovine plasma was spread over a  $1\text{-cm}^2$  area on the surface of a microscope coverslip. Excess plasma was removed to make a uniform thin layer. The coverslip was then placed under an incandescent desk lamp to dry the plasma and promote its absorption to the coverslip. An aqueous solution of thrombin (100 units/ml) was quickly applied to the dried plasma layer for several seconds, and then removed using a Pasteur pipette. The thrombin catalyzed a clotting of the plasma layer that was adsorbed to the coverslip. The coverslip was now covered with culture medium. Deyolked embryos or embryonic explant were transferred to the coverslip with a heat-polished Pasteur pipette, making sure to avoid contact of the tissues with air-water interfaces. The deyolked embryos or explanted tissue rudiments were positioned and secured on top of, or underneath, the plasma clot layer.

## Explant preparation and mounting

Desired sections of the zebrafish embryo were extirpated using sharp tungsten tools. Removal of the enveloping layer (EVL), which covers the embryo proper, was avoided, as explants quickly lost their natural morphology without the EVL or epidermis. The cut edges of the enveloping layer or epidermis often helped embryonic explants stick to the plasma clot. Using a fire polished glass Pasteur pipette, individual embryonic explants were transferred onto the plasma clot. The explants were then oriented with a blunt metal poker (sewing needle mounted in a holder), the end of fine watchmaker's forceps, or an eyelash tool. Once the explant was manipulated into the desired orientation, it was gently pressed down against the plasma layer to secure it. Additional plasma can be used to further stabilize the explant. Residual thrombin from the first plasma layer will clot the added plasma. Excessive plasma should be avoided, since it will restrain the explant and prevent normal morphogenesis. To circumvent this, plasma can be diluted prior to adding. If needed, additional culture medium can be added once the explant is immobilized. Lateral-side down and dorsal-side down explants were made somewhat differently. A small hole was opened in the plasma layer using microforceps and/or a tungsten microneedle. The plasma

clot layer was then lifted up until the clot became slightly detached from the cover slip. The explant was then moved underneath the plasma layer. Once released, the plasma clot gently pressed the explant down against the coverslip. Additional plasma can be injected under the clot to further stabilize the explant. An alternative securing medium is low-melting point agarose. A low concentration of 0.75% agarose is preferable.

# Introduction

## Zebrafish neurulation

The zebrafish serves as an excellent model organism to study vertebrate brain development. In this small teleost (bony) fish, embryonic development proceeds rapidly from fertilization to the free swimming larva within 2 days (Kimmel et al., 1995). Conveniently, the zebrafish embryo is transparent during its early developmental stages, allowing for detailed analysis of cell behavior.

Brain development in zebrafish, as in all vertebrates, starts with neural induction (see below), a process that leads to the formation of neural tissue from ectoderm. As a consequence, the neural plate forms within the embryonic ectoderm. In all vertebrate species examined, the anterior neural plate subsequently undergoes primary neurulation to form the neural tube, while the most posterior parts of the neural tube form by secondary neurulation. As opposed to primary neurulation, the formation of a neural tube from an existing epithelial sheet, secondary neurulation is characterized by a transformation of a solid rod of mesenchymal cells to an epithelial tube.

Even within primary neurulation, there are variations between vertebrate species, but the main steps are conserved: The neural plate rolls or folds up, converges, extends and finally closes to form the neural tube (fig. 1) (Colas and Schoenwolf, 2001).

Teleost neurulation has been termed secondary (Schmitz, 1993; Papan, 1994; Geldmacher-Voss et al., 2003), though evidence (Miyayama and Fujimoto, 1977; Reichenbach et al., 1990; Strahle and Blader, 1994) indicates that this is a misinterpretation (Lowery, 2004). Figure 1 illustrates the steps in zebrafish neurulation, which vary in some details from the “classical” primary neurulation:

Instead of rolling or folding up at the edges, the zebrafish neural plate sinks into the embryo to form a neural keel, a rod of neuroepithelial cells without an apparent medial opening, which, through dorsal closure, forms the neural rod. Only “secondarily”, a lumen forms in the neural rod. Although there is no

obvious rolling up of the neural plate, fate mapping indicates that the movements of the neural plate are equivalent in teleosts and other vertebrates, where initial mediolateral cell positions correspond to later dorsoventral positions in the neural tube (Schmitz, 1993; Papan, 1994) (fig. 1).

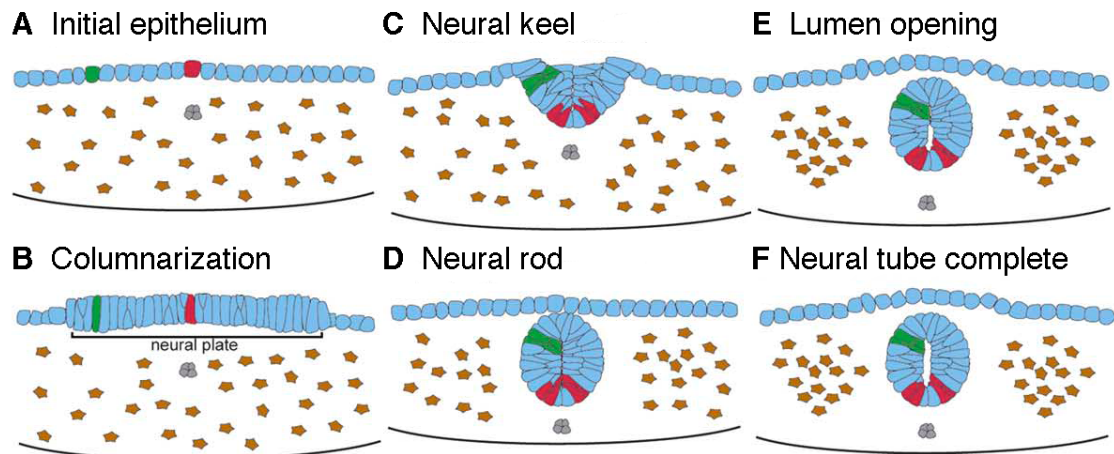


**Figure 1** Zebrafish neurulation

The zebrafish neural tube forms through the process of primary neurulation from the neural plate. Lateral positions in the neural plate (green) correspond to dorsal positions in the tube, whereas medial positions in the plate (red) correspond to ventral positions in the tube. Figure modified from Lowery and Sive (Lowery, 2004).

## Neural induction and initial neural patterning

80 years ago, Hilde Mangold's and Hans Spemann's experiments on amphibian embryos laid the foundation for the work on neural induction (Spemann, 1924). Mangold and Spemann showed that a small piece of the amphibian blastula, the dorsal blastopore lip, is able to induce a twinned embryo after transplantation to the ventral side of a host embryo. These experiments lead to the idea of the "organizer", a localized small population of cells that releases instructive signals which are able to induce and pattern surrounding tissue.

Equivalents of the Spemann organizer have been identified in all vertebrate model organisms: The mouse and chick organizers are termed node, while the teleost organizer resides in the embryonic shield.

The organizer functions in the establishment of the three body axes in all three germ layers including, therefore, anterior-posterior patterning of the induced neural tissue.

Otto Mangold discovered that the early organizer had different inductive capacities when compared to the late organizer, which was only able to induce trunk/tail structures in the host embryo (Mangold, 1933). His experiments led to the idea of a subdivision of the organizer into separate head, trunk and tail organizers.

Seemingly opposing this idea is Nieuwkoop's "activator-transformer" model, where an early activator induces general forebrain fate in the embryonic ectoderm, while subsequently acting transforming signal(s) differentially posteriorize the neuroectoderm (Nieuwkoop, 1954).

Even though many molecules secreted by the Spemann organizer have been identified since those early embryological studies, there is still no unified model for neural induction and early neural patterning (Stern, 2001), partially due to differences between amniotic and anamniotic vertebrates (Wilson and Edlund, 2001).

## Secondary neuroepithelial organizers

At the neural plate and tube stages, local signaling centers in the neuroepithelium, known as secondary organizers, refine the initial a-p specification of the brain primordium: the prosencephalon or forebrain, the mesencephalon or midbrain and the metencephalon (rhombencephalon) or hindbrain. These organizers have been termed secondary as opposed to the primary blastula stage organizers, as they form later in development (Echevarria et al., 2003).

Four regions in the neural plate and tube have been identified as (putative) secondary organizers: the anterior neural ridge (ANR) at the very anterior end of the neural plate (Shimamura and Rubenstein, 1997; Houart et al., 1998), the zona limitans intrathalamica (ZLI) in the diencephalon (suggested organizer) (Echevarria et al., 2003), the midbrain-hindbrain boundary (mhb)

(Martinez et al., 1991; Marin and Puelles, 1994) and rhombomere four (r4) of the hindbrain (Maves et al., 2002; Walshe et al., 2002).

Common to these regions in the neuroepithelium is the expression of secreted patterning molecules that direct to a large extent the development of surrounding tissue (Echevarria et al., 2003). The ANR, the mhb organizer and the putative r4 organizer all express members of the fibroblast growth factor (Fgf) family of secreted molecules, whereas ZLI cells express Sonic Hedgehog (Shh).

The mhb organizer has been particularly well studied. It displays all features of “classic” organizers: Transplantation to ectopic positions in the neuroepithelium induces non cell-autonomously midbrain and cerebellar structures, while its ablation (surgically or by genetic means) leads to a loss of structures in neighboring tissues. It has been demonstrated that mhb organizer properties can be mimicked by the Fgf family member Fgf8, while loss of Fgf8 function leads to a loss of organizer activity (Crossley et al., 1996; Meyers et al., 1998; Reifers et al., 1998; Martinez et al., 1999).

## The neuromeric model of brain regionalization

An additional model to explain how order is created within the developing vertebrate brain was already put forward by researchers in the late 19<sup>th</sup> century. A wealth of anatomical studies dealt with the occurrence of segmentally arising bulges in the neural tube, which were first described by von Baer (Baer, 1828). Almost 60 years later, Orr coined the term “neuromere” (Orr, 1887) for these structures.

Two opposing views were held by those early anatomists: First, that neuromeres are either fixation artifacts or a consequence of mechanical interactions between the neural tube and the adjacent mesoderm, and second the interpretation that neuromeres are evidence in favor of an intrinsic compartmentalization and therefore remnants of a metameric segmentation of the nervous system. As a consequence of the latter view, there was consent that neuromeres can be homologized between vertebrate species, but different views about the correct homology were put forward.

A number of researchers (Locy, 1895; Meek, 1909; Palmgren, 1921; Bergquist and Kallen, 1953; Bergquist and Kallen, 1954) came to the conclusion that the mesencephalon of a number of bony fish species examined is subdivided into two neuromeres (mesomeres), while some others, analyzing *Petromyzon* or shark species, found three (Zimmermann, 1891) or only one (Ahlborn, 1883; Neal, 1898). For the metencephalon, the number of neuromeres described varied mostly between six and eight.

There was consent, however, that the mesencephalon and metencephalon are separated by a neuromeric boundary. The vast majority of anatomists placed this boundary just rostral to the nucleus of the trochlear (fourth cranial) nerve, which lies in the anterior-most metencephalic segment. This segment, initially termed rhombomere 1 (r1), was subdivided into two rhombomeres (r0 and r1) by Vaage (Vaage, 1969), a view that is also found in the modern literature (Gilland and Baker, 1993; Waskiewicz et al., 2002). In agreement with earlier publications, Vaage (Vaage, 1969) divided the mesencephalon into two neuromeres and claimed that the second one diminishes during development and forms the boundary segment between the mesencephalon and rhombencephalon. I speculate that the posterior mesencephalic lamina (fig. 6, C-F) corresponds to this second mesencephalic segment.

As in most cases several species were examined by the authors, the differences in assignment of the boundary were most likely due to differing interpretations of the observations. With the limited techniques available, all results had to be based solely on comparative anatomical studies.

## A modern definition of neuromeres

With the advent of modern cellular and molecular biology techniques, interest in vertebrate brain compartmentalization was reinitiated in the late 80s and early 90s. This was strengthened by the progress in understanding the mechanisms of invertebrate segmentation, namely in *Drosophila* (Lewis, 1978; Nüsslein-Volhard and Wieschaus, 1980; Ingham, 1988).

Keynes and Lumsden (Keynes et al., 1990) summarized the criteria that neuromeres have to meet to be of developmental importance:

1. The neuromeric pattern should correspond to an underlying segmental pattern of cellular differentiation.
2. Patterns of cell proliferation should match the neuromeric pattern.
3. Genes with possible regulatory roles should be expressed in patterns that relate to the neuromeric pattern.
4. The boundaries between neuromeres should represent (at least transiently) boundaries for cell movement.

## The Rhombencephalon

The vertebrate hindbrain serves as a good example for the criteria stated above:

1) It was found that patterns of neuronal differentiation correspond to morphological segmentation. This is true for many different neuronal types in the zebrafish hindbrain, including reticulospinal, motor and commissural neurons (Lumsden and Keynes, 1989; Trevarrow et al., 1990; Chandrasekhar et al., 1997). The hindbrain contributes eight of the twelve pairs of cranial nerves (V to XII). It was shown that the early segmental organization of these cranial nerves is rhombomere dependent and that there is an intimate link between branchial arch innervation from these nerves and the periodicity of the branchial arches themselves (Lumsden and Keynes, 1989). Interestingly, neural crest cells migrating from the hindbrain roof and contributing to branchial arch formation also follow a rhombomere-linked periodicity (Halloran and Berndt, 2003).

2) Differential proliferation is another characteristic feature of hindbrain segmentation, as the rhombomere centers show peaks of proliferative activity, while the boundaries display a lower proliferation rate (see “specialized boundary cells”).

3) Many developmentally important genes show rhombomere-specific expression patterns, among them the *hox* genes (Lumsden and Krumlauf, 1996; Moens and Prince, 2002) and cell adhesion molecules of the Eph receptor and ephrin ligand class (see below).



4) In terms of cell behavior, the last criterion, which can be seen as the most important one, translates as follows: Cells are free to mix within a given segment, but not across the boundary to the next neighboring compartment, a process first discovered in *Drosophila* wing imaginal disc development (schematized in fig. 2) (Garcia-Bellido et al., 1973; Crick and Lawrence, 1975; Lawrence and Morata, 1976).

Lineage restriction has been shown to act during rhombomere formation. Here, clones derived from single labeled cells are free to contribute to several rhombomeres before the formation of rhombomere boundaries, but not afterwards, when they remain restricted to individual segments (Fraser et al., 1990).

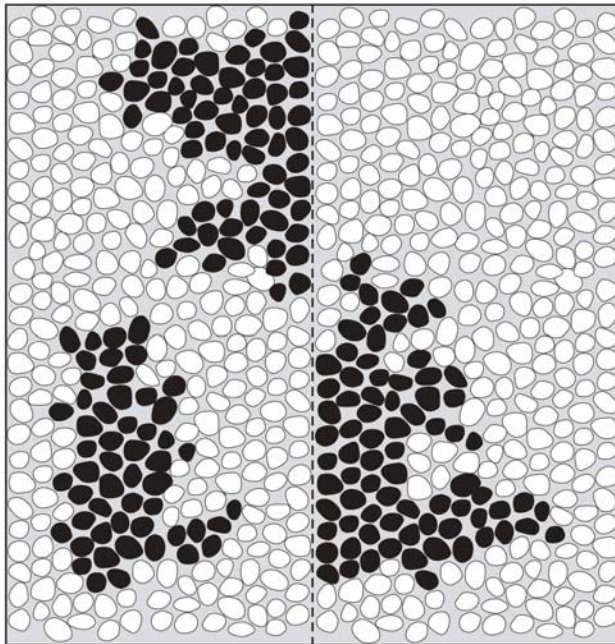


**Figure 2** Compartment boundaries can be visualized by lineage markers. During growth of *Drosophila* wing discs, cells do not move over large distances. As the plane of cell division appears to be random, patches of cells are irregularly shaped. Cells of a clone abutting a compartment boundary (dashed line) sort out from cells of the adjacent compartment giving rise to a straight and smooth clonal border. (Image and description modified from Dahmann and Basler, 1999.)

## Lineage restriction mechanisms

Although the signaling pathways that lead to the establishment of compartment boundaries in the *Drosophila* wing have largely been identified (Dahmann and Basler, 1999; Tepass et al., 2002), the mechanisms that segregate cells from each other along these boundaries are still elusive.

On the contrary, the differential adhesion hypothesis formulated by Steinberg (Steinberg, 1963) describes the general features of hindbrain segmentation (fig. 3).

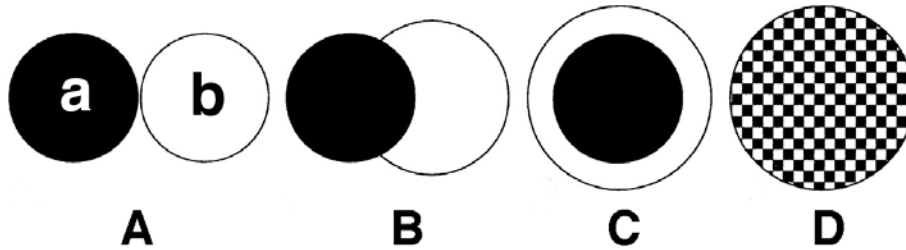


**Figure 3** The differential adhesion hypothesis.

If two populations of adhesive cells are juxtaposed (“a” and “b” cells), they will adopt configurations that depend upon the relative strength of homophilic and heterophilic adhesion (Steinberg, 1963). **A)** Without heterophilic adhesion, the cells remain separate. **B)** When the strength of heterophilic adhesion is less than either of the homophilic adhesions, the less adhesive cells will partially envelope the more adhesive cells. **C)** When the strength of heterophilic adhesion is greater than the weakest homophilic adhesion, the less adhesive cells will completely envelope the more adhesive cells. **D)** When the strength of heterophilic adhesion is greater than the average of the homophilic adhesions of the two cell populations, then the cells will intermix. (Figure and text modified from Irvine and Rauskolb, 2001.)

Work in zebrafish identified the large family of Eph receptors and ephrins (Holder and Klein, 1999; Kullander and Klein, 2002) as mediators of differential adhesion between rhombomeres. In two articles published in 1999, Wilkinson and co-workers demonstrated that the expression of ephrin ligands and Eph receptors in adjacent cell populations is sufficient to mediate differential adhesion (Mellitzer, 1999), and that cells overexpressing either ligand or receptor sort to rhombomere boundaries in live zebrafish embryos (Xu, 1999). Later, upstream factors for the regulation of ephrin and Eph expression in specific rhombomeres were identified (Moens et al., 1998; Cooke et al., 2001). These key experiments were preceded by the findings that Eph receptors and ephrins are expressed in complementary rhombomeres (Nieto et al., 1992; Xu and Wilkinson, 1997) and that odd- and even-numbered rhombomeres display different adhesive properties (Guthrie et al., 1993; Wizenmann and Lumsden, 1997).

For compartments to form developmental units, lineage restriction between neighboring segments appears to be of prime importance and is the key criterion for true neuromeres.

An alternative (or partially redundant) mechanism to maintain sharp gene expression boundaries and defined cell populations is plasticity (fig. 4). Here, cells leaving a certain developmental compartment are reprogrammed to the target compartment’s expression profile and fate. It was shown by extensive

single cell injection and clonal analysis, that a small number of hindbrain cells violate the lineage restriction boundaries between rhombomeres in the chick (Birgbauer and Fraser, 1994). An as yet unknown mechanism based on plasticity has to act on these cells to maintain sharp gene expression interfaces.

Experiments performed both in mouse and zebrafish (Trainor and Krumlauf, 2000; Schilling et al., 2001) have shown that cells can indeed be reprogrammed to their target tissue's genetic program in the vertebrate hindbrain and neural crest. Interestingly, the degree to which cells could be altered in terms of their gene expression profile depended on community effects: Small numbers of cells or isolated cells were more likely to be reprogrammed than larger groups. This finding argues that the small number of isolated cells that escape the rhombomere lineage restriction is likely efficiently reprogrammed.

At not lineage restricted boundaries in the embryo, plasticity may be the main mechanism that maintains separate identities of neighboring tissues.

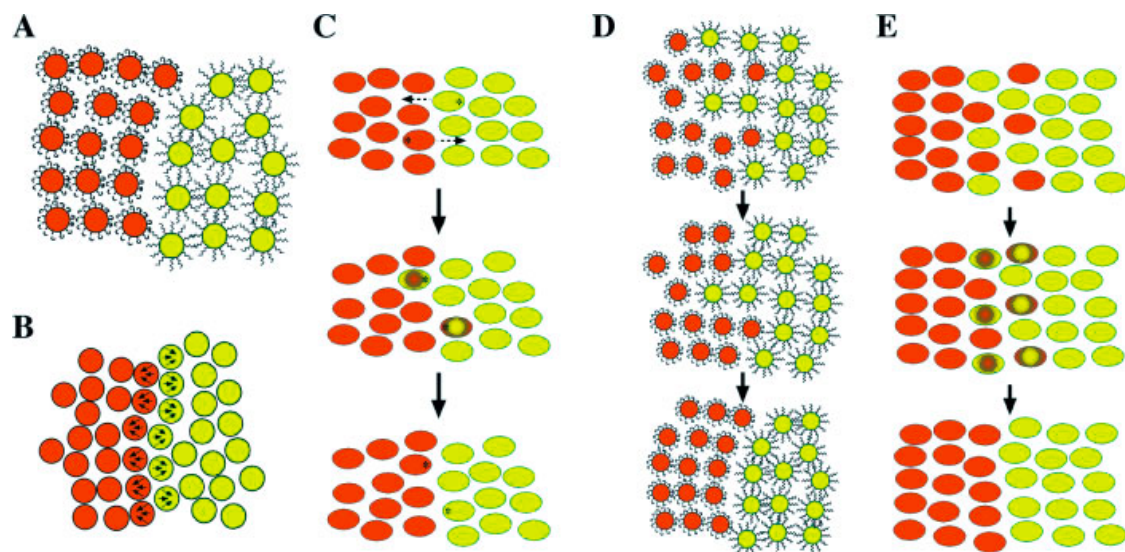


**Figure 4** Mechanisms to establish and maintain sharp interfaces between adjacent cell populations. **A-C)** Two general mechanisms can maintain interfaces: A,B: Homophilic adhesion (A) and/or mutual repulsion (B) due to differential adhesion or (C) plasticity: Identity switching of cells that crossed the interface. **D,E)** These same two mechanisms can be used to sharpen boundaries between two initially mixed cell populations either by local cell sorting (D) or by cell-identity switching (E). (Figure and description modified from Pasini and Wilkinson, 2002.)

## More compartments in the vertebrate brain?

It is as yet unclear whether the anterior neural tube is compartmentalized in general, similar to the rhombencephalon. Rather, lineage restriction boundaries have so far only been identified framing the zona limitans intrathalamica (ZLI) (Larsen et al., 2001), at the diencephalon-mesencephalon (di-mes) border (Larsen et al., 2001; Zervas et al., 2004) and at the mhb (this study and Zervas et al. (Zervas et al., 2004)). Lineage restriction studies at the mhb will be discussed in more detail.

## Specialized boundary cells

The cells forming rhombomere boundaries acquire distinct properties during development. Källén described peaks of proliferative activity in the center of neuromeres, while the boundaries were characterized by lower proliferation (Källén, 1962). These findings were confirmed by Guthrie et al.: Within rhombomeres, S-phase nuclei were located predominantly towards the pial (outer) surface of the neuroepithelium, while at rhombomere boundaries S-phase nuclei were significantly closer to the ventricular (inner) surface. The density of mitotic figures was greater toward the centers of rhombomeres than in boundary regions (Guthrie et al., 1991).

Furthermore, rhombomere boundary cells are characterized by larger intercellular spaces than between cells in the adjacent neuroepithelium, a distinct extracellular matrix and the expression of specific genes (Lumsden and Keynes, 1989; Layer and Alber, 1990; Moens and Prince, 2002). It has not been analyzed so far whether other lineage boundaries in the vertebrate brain possess these special properties.

## Lineage restriction and organizers

Lineage restriction boundaries have first been shown to coincide with the position of organizers that pattern the surrounding tissue in insect development (Dahmann and Basler, 1999).

The position of potent organizing cells has to be highly controlled; otherwise tissue formation and differentiation will be impaired (fig. 5). A mechanism to segregate a cell population expressing an organizing molecule from non-expressing cells leads to a sharply defined boundary between the two groups. This way, a precise patterning of adjacent tissue is ensured.

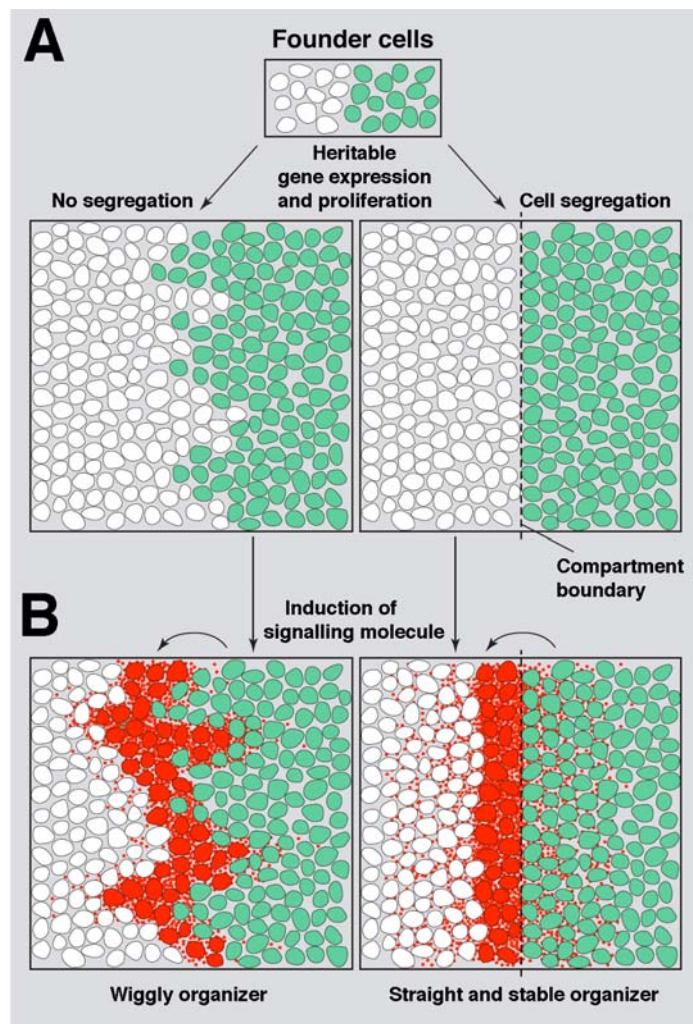


**Figure 5** Organizers and lineage restriction boundaries.

**A)** A tissue is subdivided into two founder cell populations that differ in the expression of a “selector” gene. Its expression becomes heritable and the two populations proliferate, which leads to an intermingling between them. By establishing a cell segregation system (right panel), the border between the two cell populations remains straight.

**B)** The selector gene drives the expression of a signaling (organizing) molecule (red) in the neighboring cell population. A wiggly border between expressing and non-expressing cells leads to an unstable organizer incapable of directing precise patterning (left panel). In contrast, the compartment boundary leads to a straight and stable organizer and thereby to a precise patterning of the tissue (right panel). (Image and description modified from Dahmann and Basler, 1999.)

As discussed, such organizers also play important roles during vertebrate brain development.

The mhb organizer has been subject to lineage restriction analyses in two vertebrate species with controversial results. In the chick, the question remains open (Millet et al., 1996; Jungbluth et al., 2001; Louvi et al., 2003). A recent study, based on a genetic labeling approach, suggests the existence of several lineage boundaries at the mhb in the mouse (Zervas et al., 2004).

Combining the neuromeric model of brain formation and the concept of secondary organizers, it can be suggested that organizing cell populations are framed by segment boundaries. This holds true for the r4 organizer and the ZLI, while it is not clear whether the mhb organizer cell population is separated from the surrounding tissue by lineage boundaries.



## Embryonic explants

Interest in developing an explant technique for zebrafish embryonic body parts was initiated by the observation that the mhb region folds up during a period of strong morphological changes (see main introduction).

Several mechanisms to bring about such a folding can be envisioned:

- During zebrafish development, the angle between body and head decreases (Kimmel et al., 1995), leading to a straightening of the embryonic axis. It is possible that this upward movement of the head exerts pressure onto the neural tube, forcing it to fold.
- At around the 18-somite stage, the brain ventricles start to fill with fluid and increase more and more in size. This increase in ventricle volume may “inflate” the brain and contribute to the folding.
- Folding of the neural axis may be a local, cell intrinsic program: Changes in cell shape can contribute to epithelial morphology in many ways (Ettensohn, 1985; Colas and Schoenwolf, 2001).

Explanting the developing zebrafish head would test the first two mechanisms, as a removal of the body will release the head of putative pressure from the decrease of the angle between body and head. Furthermore, a mechanism that “inflates” the head through pressure from the ventricle fluid is hard to imagine in a scenario where the neural tube is cut open.

Apart from addressing the mechanism of the mhb folding process, an explant system may serve imaging studies in the zebrafish. Extended time-lapse recordings of zebrafish embryos are often disrupted by spatial movements associated with the extension and straightening of the embryonic axis, as well as movement artifacts associated with developing musculature. Moreover, the embryo's massive yolk cell often prevents easy optical access to tissues of interest. One direct way of dealing with these difficulties is to physically remove the yolk cell and isolate tissues of interest in the form of embryonic explants.

Here, I will show that head explants of zebrafish embryos develop almost normally in culture for up to at least 24 hpf, which opens up a number of potential applications.



# **Aim of the thesis**

**I: Is the midbrain-hindbrain boundary in zebrafish a lineage restriction boundary?**

1. Do we see the establishment of a lineage restriction boundary between the midbrain and hindbrain? And, if yes:
2. When is this lineage boundary established?

**II: What is the mechanism behind the observed lineage restriction?**

1. Does the lineage restriction boundary correlate with genetic markers and morphological subdivisions?
2. Which of the genes expressed in the mhb might be responsible for setting up the lineage restriction boundary?

**III: Are there more compartment boundaries in the mhb area?**

To address these questions, the aim of this thesis was to establish a method allowing me to continuously follow the movement of cells in the developing mhb region with cellular resolution over extended time periods and to correlate cell behavior with regional gene expression and anatomy.

Finally, I sought to identify molecular players involved in the putative lineage restriction mechanism.

# Results

## Lineage restriction at the midbrain-hindbrain boundary

### Morphological changes during midbrain-hindbrain boundary formation

To introduce zebrafish mhb development, I show normal stages of its formation and illustrate the connection between morphological changes and gene expression patterns. These data are in part taken from my Diploma thesis (Langenberg, 2000) and from the Diploma thesis of Silke Schmitt (Schmitt, 1999). I reproduced the gene expression data to obtain a better image quality and to extend the analysis to earlier stages.

To visualize mhb formation, I stained a series of live embryos with the vital dye Bodipy-ceramide (Cooper et al., 1999) and took dorsal and lateral confocal optical sections of the brain (fig. 6 A-F).

Up to about the 12-somite stage, the putative mhb region of the neural tube shows no overt signs of morphological segmentation (fig. 6 A). During the formation of the next 2-4 somites, an indentation starts to form in the prospective mhb region (fig. 6 B, arrowheads). This indentation successively deepens and widens as the neural tube goes through a drastic change in morphology at the level of the mhb. Both the midbrain tectum and the hindbrain cerebellum strongly proliferate and bulge laterally. Furthermore, the neural tube folds up along its anterior-posterior (a-p) axis (dotted line in B). As a consequence of these processes, the cerebellum pushes slightly anterior into the midbrain so that the morphological boundary between the midbrain tectum and hindbrain cerebellum becomes tilted with respect to the a-p axis of the embryo (dashed line in C, compare to panels H-K and fig. 10). At 24 hours post fertilization (hpf), between the prominent tectum opticum and the cerebellum, at the hinge point of the folded mhb region, the posterior mesencephalic lamina becomes distinguishable (asterisk in fig. 6 C-F).

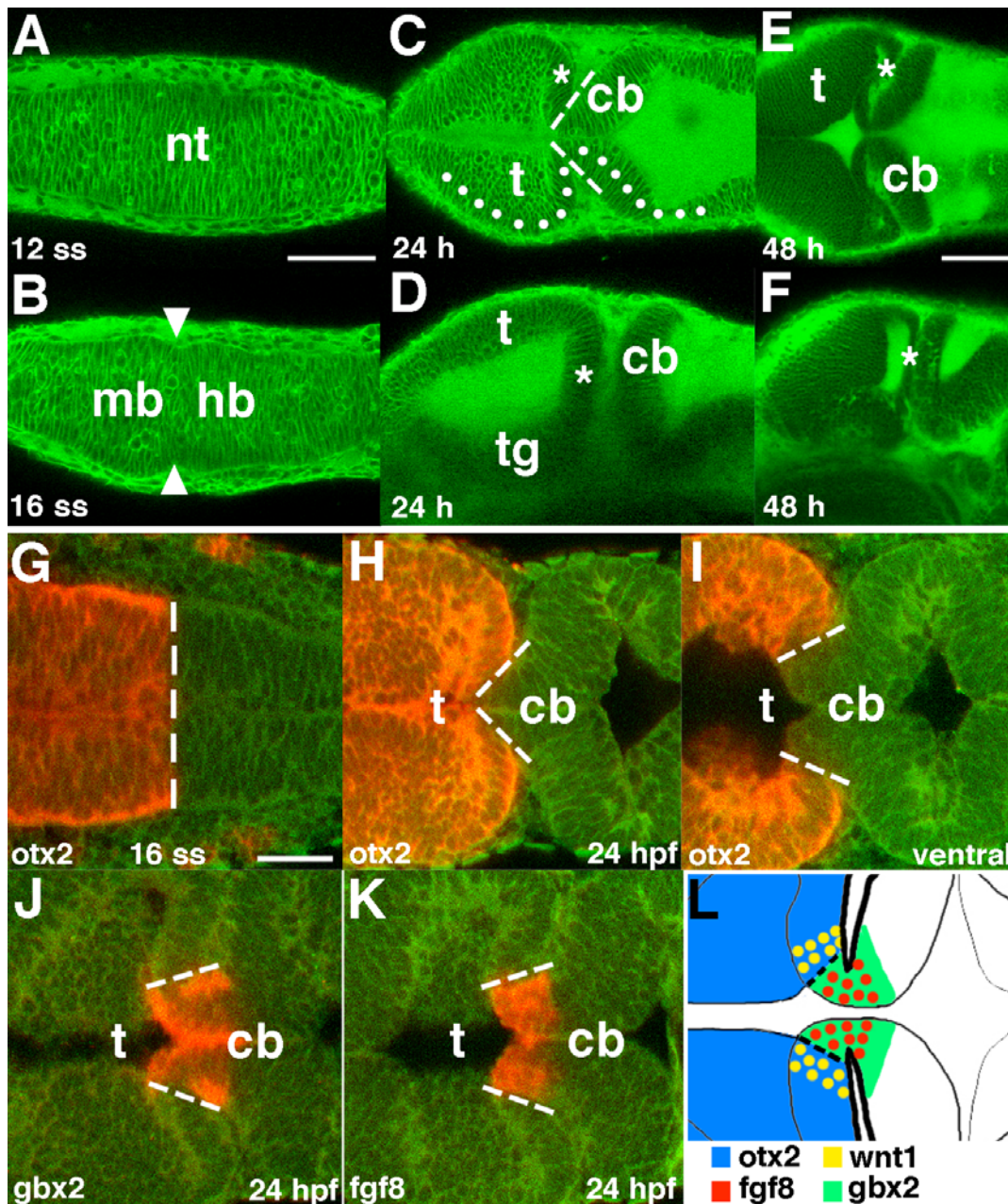


**Figure 6** Morphological changes during mhb formation

**A-F)** Confocal optical sections of live embryos, stained with Bodipy-ceramide. From the 12- (A) to the 16-somite stage (B), a small indentation forms in the neural tube (nt) at the level of the prospective mhb (B, arrowheads). At 24 hpf (C, D), the now very deep invagination clearly separates the midbrain tectum (t) from the hindbrain cerebellum (cb). The a-p axis has folded up in the mhb area (dots in C). From 24 hpf onwards, a posterior mesencephalic lamina (pml) is visible in the very posterior midbrain (asterisk in C, D). This structure is prominent up to at least 48 hpf, when it is found squeezed in between the tectum and cerebellum (asterisk in E, F). **G-I)** Confocal optical sections of fixed embryos stained for *otx2* expression in red. The posterior gene expression boundary reflects morphological changes. Ventrally, it becomes broader (compare to H to I). **J,K)** The expression domains of *fgf8* and *gbx2* seem to fit within the gap in the *otx2* expression domain at 24 hpf. **L)** Summary scheme of gene expression domains at 24 hpf. Dots indicate co-expression, the mhb is marked by a hatched line. All images are dorsal views, except D,F: lateral views; anterior is to the left. Dashed lines indicate the position of the mhb. Scale bars = 50 microns (A applies to A-D, E to E+F, G to G-K).

This structure remains only one cell row wide up to at least 48 hpf (fig. 6 E,F). Movie A on the accompanying CD further illustrates morphological changes during mhb formation (see movie description at the end of the thesis).

To address the correlation between morphological changes and gene expression in the mhb region, I stained various embryonic stages with *in-situ* probes against *otx2*, *gbx2*, *fgf8* and *wnt1* and took dorsal confocal optical sections of fixed specimens (fig. 6 G-L). *Otx2* is a canonical midbrain and forebrain marker gene (Simeone et al., 1992; Mori et al., 1994; Bally-Cuif et al., 1995b), while it has been demonstrated that *wnt1* expression lies within a posterior stripe of the *otx2* domain (Wilkinson et al., 1987; Molven et al., 1991; Hidalgo-Sanchez et al., 1999a), marking the posterior most part of the midbrain. *Gbx2* is one of the two *gbx* homologues in the zebrafish, whose anterior expression border marks the anterior most extent of the hindbrain (Wassarman et al., 1997; Niss and Leutz, 1998; Rhinn et al., 2003). *Fgf8* expression is contained within an anterior stripe of the *gbx1* domain (Crossley and Martin, 1995; Reifers et al., 1998; Hidalgo-Sanchez et al., 1999a; Rhinn et al., 2003).

As in the living embryo, the earliest time when the morphological constriction can be observed is between the 12- and 16-somite stage. Due to the fixation process, this is not as clear as in the live samples, therefore, it cannot be judged whether the gene expression boundary and morphological boundary coincide at this stage. At 24 hpf, the *otx2* gene expression domain clearly lies within the constriction and is tilted with respect to the embryo's a-p axis (dashed line in H,I). Interestingly, both *otx2* and *wnt1* (data not shown) leave a gap in their expression domain, whose extent varies from dorsal to ventral (Schmitt, 1999). At all dorsal-ventral levels, the gap is filled by *gbx1/2* and *fgf8* expression, such that their anterior expression borders abut the posterior borders of *otx2* and *wnt1* (Schmitt, 1999) (fig. 6 J,K). Figure 6 L summarizes gene expression domains at the mhb at 24 hpf.

## Behavior of individual cells

To analyze the behavior of individual cells during the folding process, I transplanted cells expressing cytosolic GFP from injected donor embryos into the putative mhb region of unlabeled wild-type hosts at the shield stage (onset of gastrulation, 6 hpf) (Woo and Fraser, 1995), and imaged the developing mhb region by spinning disc confocal microscopy between the 5-somite stage (11.5 hpf) and 30 hpf (fig. 7 and movie B). Embryos were imaged with a time interval of 10 min and over multiple z-planes. This enabled me to follow individual groups of cells continuously over the whole imaging period.

In summary, cells showed very dynamic interkinetic movements and divided readily in all 13 acquired movies (fig. 7 and movie B). Despite their high motility, cells displayed relatively little movement along the a-p axis of the embryo. From these observations I can conclude the following:

- The local folding of the a-p axis at the mhb is not brought about by movements of individual cells, but is rather a rearrangement of whole tissue parts.
- In all analyzed movies, I was able to trace groups of cells divided by the morphological boundary back to separate cells or cell groups at the beginning of the time-lapse (fig. 7, pseudo-colored red and yellow cells and movie B). I take this as a first indication of lineage restriction between the midbrain and anterior hindbrain.

Movie B illustrates cell behavior during the mhb folding process.

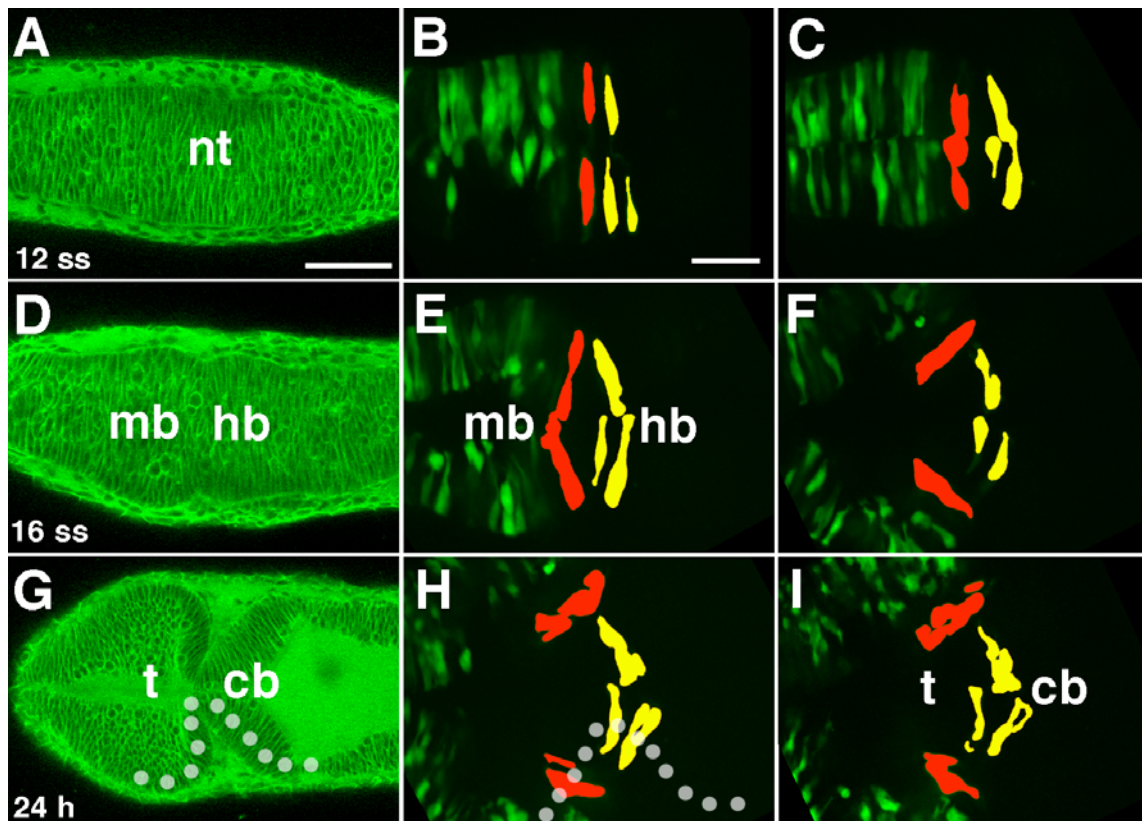


**Figure 7** Time lapse confocal microscopy reveals behavior of individual cells.

**A,D,G:** Confocal sections of Bodipy-Ceramide stained embryos at the indicated stages (see introduction). **Other panels** show stills from one time lapse, the middle column corresponds approximately to the stage in the left most column. Pseudo-colored red cells were situated in the midbrain tectum, yellow cells in the hindbrain cerebellum at the end of the movie (I) and were backtracked to the beginning (B). A gap forms between the two cell groups and grows with time. Cells can be seen to divide and to be oriented along the folded a-p axis of the embryo (dotted line in G+H). There is no mixing between the two colored cell groups, but seemingly also little mixing within them. All images dorsal views, anterior to the left. Developmental time increases from A to I. nt – neural tube; mb – midbrain; hb – hindbrain; t – midbrain tectum; cb – cerebellum; Scale bar = 50 microns in A (applies to left column), 25 microns in B (applies to middle and right column).

## Lineage label by Dil application

To challenge a putative lineage restriction mechanism at the mhb, I bulk labeled cells at the mhb by shortly inserting a Dil-coated glass capillary into the prospective mhb region of a living zebrafish embryo at the 5-somite stage (fig. 8 A) and documented the position of labeled cells up to at least 36 hpf. Dil is a strong lipophilic dye that is known to label cell membranes. Daughter cells of the originally labeled cell population will inherit the marker through division, but unlabeled cells will not acquire it, as the dye does not unspecifically diffuse between cells.

Out of 18 cases with a label near the mhb, 15 were confined to one side of the boundary at 36 hpf, 2 were two-sided and one case could not be resolved (fig. 8 B-E). This confinement could be observed despite a large number of cells carrying the label (fig. 8 C,E).

In summary, even though many cells were marked by the Dil application, a spreading of labeled cells across the mhb was rarely observed. I take this finding as a further indication that the midbrain and hindbrain are separated by a lineage restriction boundary.

## Single cell lineage analysis by iontophoretic injection

In the zebrafish, the expression domains of the transcription factors *otx2* and *gbx1* (the functional homolog of *gbx2* in the mouse) become mutually exclusive at the 80% epiboly stage (Rhinn et al., 2003). As these genes are crucial for positioning the mhb (Rhinn and Brand, 2001; Wurst and Bally-Cuif, 2001; Raible, 2004), I expected this period to be also important for cell behavior at the *otx2/gbx1* interface.

To find the onset of the lineage separation and to obtain a single cell read out, I labeled individual cells by iontophoretic injection at successive gastrulation stages (fig. 8 F-L). In addition, I transplanted single cells from GFP injected donors to wild-type unlabeled hosts at the shield stage. Transplantations were not carried out beyond the shield stage for technical reasons.



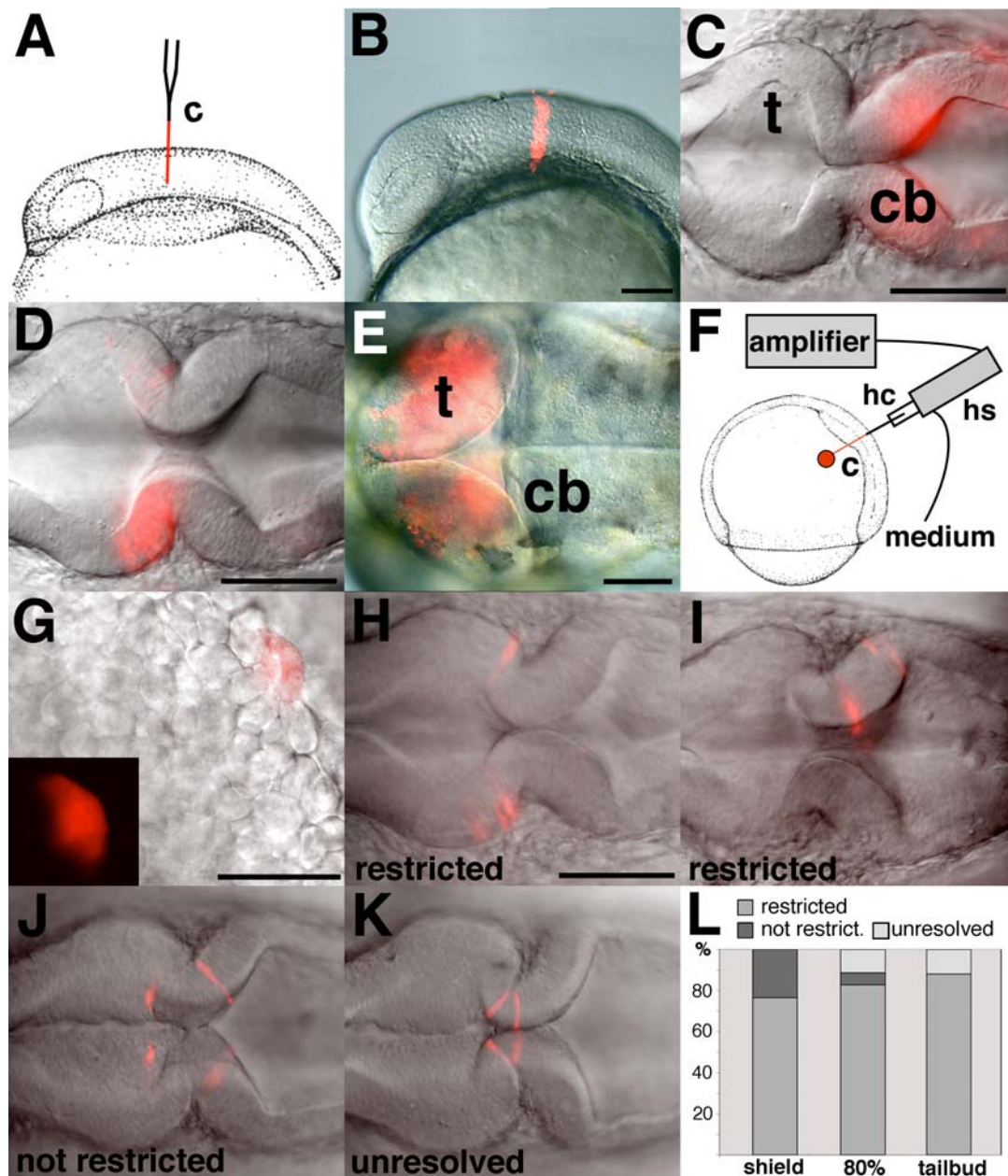


**Figure 8** Bulk labeling and injection of single cells at the mhb.

**A)** Schematic drawing of the Dil labeling procedure: A Dil coated glass capillary is shortly inserted into the prospective mhb area of the 5-somite stage embryo. **B)** An embryo 2 h after labeling with a column of labeled cells throughout the neural tube. **C-E)** Dil positive cells remain confined to one side of the mhb at 24 hpf (C, D) and up to 60 hpf. **F)** Schematic drawing of iontophoretic single cell injection: Current flows through an Ag/AgCl half-cell (hc), a dye-filled capillary (c), by ion-flow into the target cell, through the embryo, medium and to the amplifier's headstage. Current intensity is controlled via the amplifier. **G)** A single filled cell at the shield stage, inset shows the fluorescent signal alone. **H, I)** Embryos at 24 hpf bearing labeled cells on one side of the mhb, the midbrain or cerebellum, respectively. **J)** An embryo with a clear two-sided label at 24 hpf. **K)** Individual cases could not be resolved on the morphological level when cells were located directly within the boundary region. **L)** Summary chart of single cell injections and transplantations. Notice the decrease of two-sided clones from shield stage ( $n=11/47$ ), 80% epiboly ( $n=2/35$ ) to tailbud stage ( $n=0/25$ ). Shield stage statistics show a combination of single cell injections and transplantations. A and B are lateral views, C-E and H-K are dorsal views, anterior is to the left. Scale bars=100 microns, except for G=50 microns (C applies to C+D, H applies to H-K). t – midbrain tectum cb–cerebellum.



Clonal distribution was determined at 24 hpf (fig. 8) and 36 hpf (data not shown).

Upon labeling or transplanting at shield stage to 60% epiboly, I obtained about a quarter of clones with cells on both sides of the boundary at 24 hpf and 36 hpf, in agreement with earlier fate mapping studies (Woo and Fraser, 1995) (fig. 8 J). The proportion of two-sided clones decreased significantly when cells were injected during later gastrulation stages (80-90% epiboly and tailbud to 1-somite stage, fig. 8 H,I), with no clear two-sided clones after labeling at the tailbud stage (summary fig. 8 L).

These findings are a good indication for the establishment of a lineage restriction boundary between the prospective midbrain and hindbrain already at late gastrulation stages, during the period of the separation of the expression domains of *otx2* and *gbx1*.

## Clone size and clonal spread after single cell injections

Table 1 illustrates the growth and spreading of clones up to 24 hpf, derived from single cell injections at 80% epiboly and tailbud stage.

Even though the neuroepithelium goes through a period of strong morphological changes (see fig. 6) between the end of gastrulation and 24 hpf, clones only dispersed on average over eight (80% epiboly injection) and five (tailbud injection) cell diameters, respectively. Cells divided up to three times during this period.

Table 1: Clonal size and spread after single cell injection.

	<b># cells at 24 hpf</b>	<b>a-p spread at 24 hpf [μm]</b>	<b>cell width [μm]</b>
<b>80% epiboly (n=41)</b>	5.0 +/- 1.6	45.0 +/- 21.0	5.5 +/- 0.6
<b>tb to 1 somite (n=27)</b>	4.0 +/- 0.8	26.0 +/- 8.7	

The table shows the number of cells derived after single cell injection at 80% epiboly and tailbud and the distance over which these cells spread along the a-p axis of the embryo at 24 hpf. The average cell width at 24 hpf was 5.5 microns, therefore, clones spread over eight and five cell diameters on average, respectively. tb: tailbud stage

## Imaging of individual nuclei

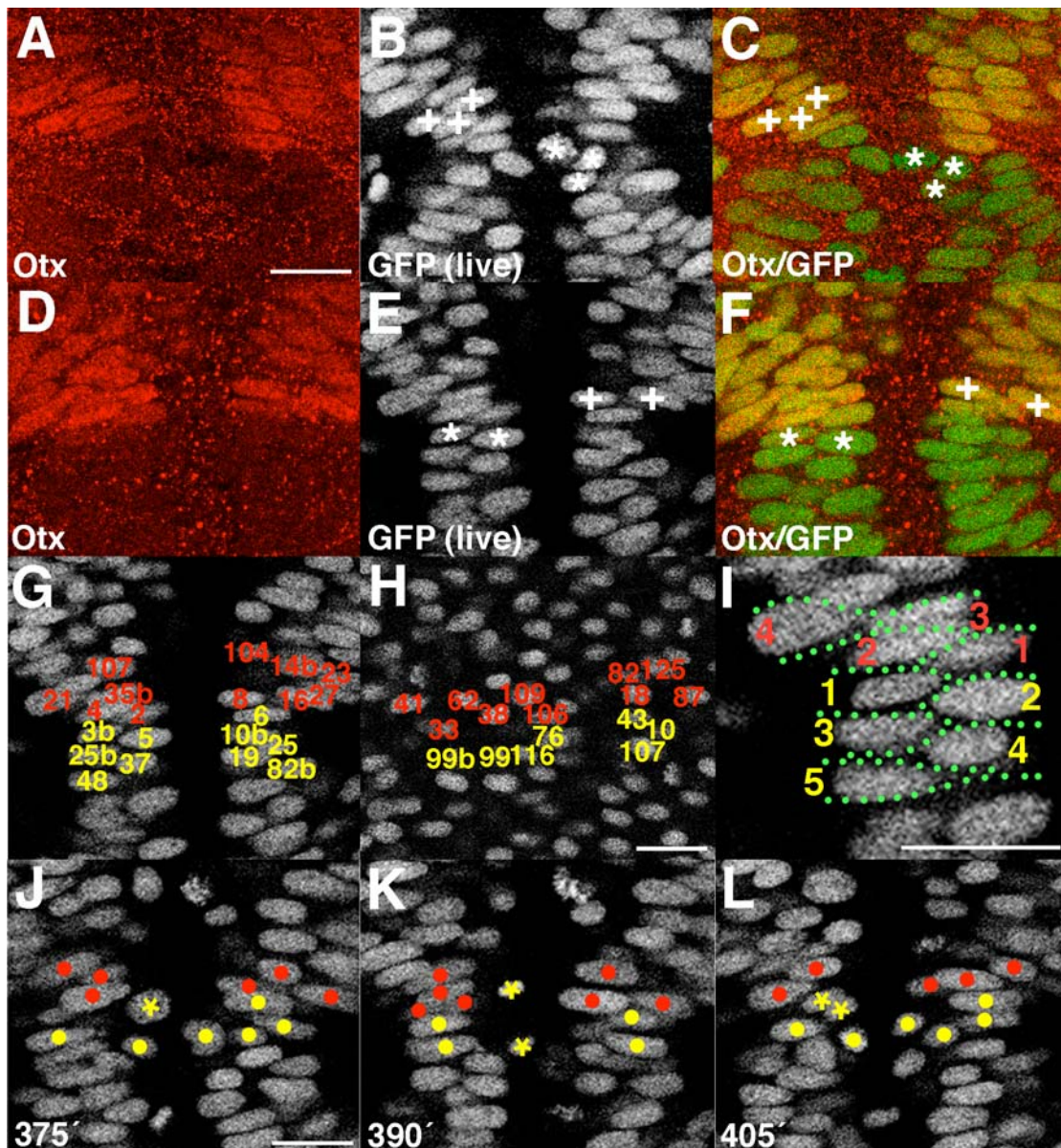
The results obtained so far argue for the existence of a lineage restriction boundary between the mesencephalon and rhombencephalon. However, the readout relied solely on morphology, with no link to the molecular status of the analyzed clones. Furthermore, the production of informative cell clones was restricted by the low a-p spread and limited growth of the clones (table 1). Therefore, to obtain single cell readout with the link to a molecular marker, I devised a high throughput imaging approach with subsequent antibody staining for the midbrain marker protein Otx. To this end, I imaged the developing mhb region in the histone H2A.F/Z:GFP fusion line (Pauls et al., 2001) with a very close z (1.5 microns) and time interval (3-4 min) on a 2-photon confocal microscope for 8 to 12 h (movie C). In this transgenic line, every nucleus is labeled by a histoneGFP fusion protein and readily distinguishable from neighboring nuclei when imaged with high numerical aperture objectives. During the imaging time, embryos developed from the 5- to 10-somite stage to the 24- to 26-somite stage (21-22 hpf, depending on the room temperature and imaging time, table 2) and cells divided up to two times.

Figure 9 illustrates the approach: After imaging, embryos were fixed in PFA, stained for Otx protein (fig. 9 A,D), and optically sectioned on a confocal microscope. By comparing the last image stack of the time lapse with the antibody staining (fig. 9 B,C,E,F), I was able to assign a molecular status

(midbrain or non-midbrain = anterior hindbrain) to the nuclei, which were then backtracked through the time lapse and their position (xy center and z-level) was noted in intervals of about one hour. Initially, I focused on the first three cell rows anterior and posterior to the Otx interface at the end of the time lapse, but this was not sufficient to cover all nuclei at the boundary at the start of the movie. Therefore, the remaining nuclei, comprising about 40% of all tracked nuclei, were tracked forward in time and their molecular status was again assigned at the end.

With this approach, I was able to assign a fate to and follow nearly all cells near the boundary (table 2).

Two-photon microscopy is known for its superior resolution in thick tissues and the low amount of photodamage (Denk et al., 1990; Small et al., 1999). Consequently, out of the forward tracked cells, only two died during the imaged period, even under nearly continuous scanning. Furthermore, imaged embryos displayed a normal morphology with only minor distortions due to the agarose embedding procedure. This argues that the imaging method did not harm the embryo.



**Figure 9** Single nucleus tracking procedure.

**A-F)** Matching of antibody staining and time lapse. **A-C)** movie 3; **D-F)** movie 1; **A, D)** Anti-Otx antibody staining; **B, E)** One plane of the last live imaging stack of a time lapse. Nuclei can be identified in both the live image and the corresponding antibody staining (**C, F**): Otx positive nuclei are marked by plus signs, Otx negative ones (only histoneGFP positive) are marked by asterisks. **G,H)** Individual nuclei are assigned a status (**G**, red = Otx positive; yellow = Otx negative), numbered and tracked backwards to the start of the time lapse (**H**). **I)** Cell position can be determined in rows distance from the Otx interface. **J-L)** Stills from one of the movies, showing an Otx negative cell that divides (asterisks) near the Otx boundary. One of the daughter cells moves into the Otx positive domain (**K**), but sorts back into its original domain (**L**). All panels show dorsal views, anterior is to the top. Scale bars=20 microns (**A** applies to **A-G**, **J** to **J-L**).

## The mhb is a lineage restriction boundary

Table 2 summarizes the results obtained from nuclei trackings in three independent embryos. Given are the numbers of nuclei tracked from the beginning of the time lapse to the end, split up into Otx antibody staining positive and negative nuclei. As is evident from table 2, the vast majority of nuclei were tracked successfully throughout the time lapse. Some were lost or excluded for one of the following reasons:

1. Movement out of focus: Due to technical limitations (e.g. the scanning speed of the 2-photon microscope), only a limited number of optical sections (40 - 50 = 60 – 75  $\mu\text{m}$ ) were acquired at each time point. As the neural plate folds up during zebrafish development, lateral cells of the plate come to lie in dorsal locations at later stages. When backtracking these cells, several moved ventro-laterally out of the last optical section and could therefore no longer be followed. This happened almost only during the analysis of the first, longest movie, which started at the earliest stage.
2. Exclusions: A small number of nuclei were repeatedly tracked onto each other (i.e. non-daughter cells ended up on the same founder cell upon backtracking). These nuclei had to be excluded from the analysis. Other nuclei were lost when they moved too quickly to be followed and mixed with other, non-tracked nuclei. However, this was very rare.
3. Neural crest cells: Some very dorsally located nuclei moved very rapidly through the neuroepithelium, most of which left it during the time lapse. These nuclei had a rounder, not as elongated shape and were more loosely packed in comparison to the rest of the neuroepithelial cells. I assume that these were nuclei of neural crest cells and did not include them in the final number of successfully tracked cells (see discussion).

Table 2: Nuclei tracking overview

Movie	time covered	Otx positive		Otx negative		Out of focus	Lost / excluded	Neural crest
		start	end	start	end	end*	end*	end*
<b>1 (12 h)</b>	5-24 ss	57	129	53	131	38	34	20
<b>2 (10 h)</b>	8-26 ss	36	66	28	56	1	0	2
<b>3 (08 h)</b>	10-25 ss	56	77	51	94	3	2	0
<b>total</b>		149	272	132	281	42	36	22
<b>restricted</b>		<b>149</b>	<b>272</b>	<b>131</b>	<b>279</b>	-	-	-
<b>not restricted</b>		<b>0</b>	<b>0</b>	<b>1</b>	<b>2</b>	-	-	-

Out of the successfully tracked nuclei, nearly 100% were found within the lineage restricted populations. In movie one, a higher number of nuclei could not be tracked to the very beginning because of their strong dorsal-ventral movement. However, these nuclei did not leave their respective groups during the time I followed them.

out of focus – nuclei that moved ventrally out of the imaging area; lost/excluded – nuclei that could not be tracked or were repeatedly tracked onto each other; neural crest – putative neural crest cells, located very dorsally and leaving the neuroepithelium during the time lapse.

\* Only the final number of nuclei is given.

To visualize the position of all tracked nuclei of a given movie simultaneously, I plotted nuclei coordinates in three dimensions (see materials and methods) and exported lateral and dorsal views from these three-dimensional plots. Dorsal views are therefore projections along the z-axis, lateral views are projections along the y-axis of the original three-dimensional plots. Figures 10 and 11 show the locations of nuclei at the start and the end of movie 1. Time points between the start and the end are not shown, but are identical in terms of the conclusions that can be drawn:

In all three movies and at every analyzed time point, Otx positive and Otx negative nuclei formed a coherent group with minimal to no overlap (fig. 10 A,B for a dorsal, fig. 11 A,B for a lateral view, respectively). The term “coherent” is used here to describe a group of cells whose members are organized in such a way that none of its members is ever separated by cells of the neighboring group from its own group members. This means that at the Otx interface, the nearest neighbor to the anterior of an Otx positive cell is always another Otx positive cells, while the nearest neighbor of an Otx negative cell to the posterior is always another Otx negative cell. During cell

division, nuclei momentarily left their respective groups to divide at the midline (fig. 9 J-L).

In contrast, nuclei of arbitrarily defined boundaries in the midbrain or cerebellum did not sort out into coherent groups (fig. 10 E,F; 11 E,F). At these arbitrary boundaries, even after trying to “optimize” for low cell mixing, I consistently found violation of the artificial boundary by 20-30% of all tracked cells. Optimizing refers to a procedure where I tried to minimize mixing by repeatedly assigning individual cells to the respective other group and plotted the final position again. Daughter cells were always assigned the same status during this procedure.

Likewise, upon shifting the Otx “border” by one cell row posterior or anterior at the beginning of the time lapse, the sharply defined interface was lost (fig. 10 C,D, 11 C,D). This demonstrates that the behavior of cells forming the mhb is specific to this boundary and that the observed lineage restriction is not due to a general behavior of cells in the mhb area.

Figure 12 A,B further illustrate the behavior of cells near the mhb: I determined the position of Otx positive and Otx negative nuclei in rows distance from their common boundary at the start and at the end of the time lapse (with the rows making up the interface receiving the number one, fig. 9 I). This is possible because the neuroepithelial cells form a pseudo-stratified epithelium at these stages (Papan, 1994; Concha and Adams, 1998), i.e. cells stretch from the apical to the basolateral surface, while the nuclei can be found at all intermediate positions, giving the appearance of a multi-layered epithelium.

By plotting the difference between the row values, one can see the relative movement of cells with respect to the boundary: Only a fraction of the cells moved towards the boundary, the vast majority moved away from it or remained stationary.

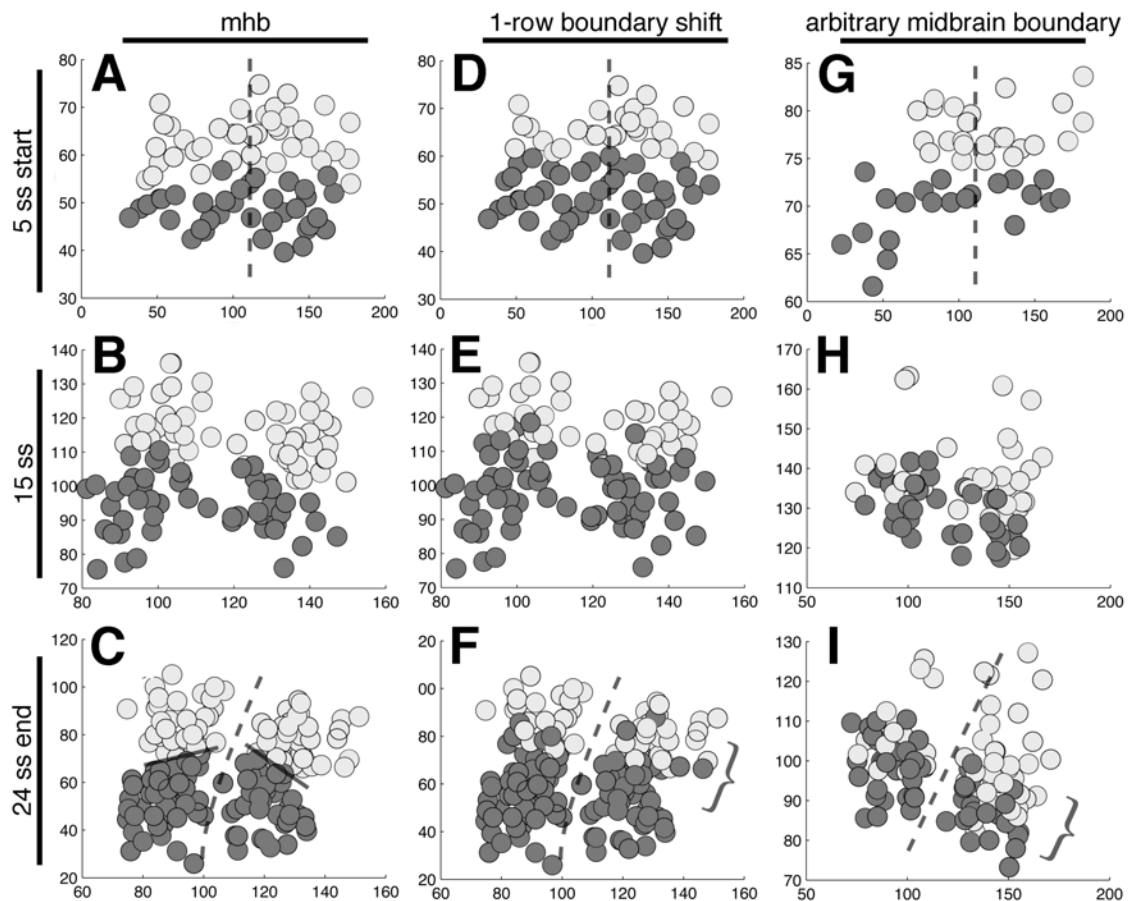


**Figure 10** Summary plots of nuclei positions I.

Otx positive nuclei are light, Otx negative nuclei dark grey. **A-C)** Otx positive and negative nuclei form coherent groups during the time lapse. Lines in C indicate the mhb, compare to fig. 6. **D-F)** Upon shifting the Otx / Otx negative interface artificially by about one cell row at the 5-somite stage (D), the sharp interface of the two cell populations is lost at later stages (E,F) The bracket indicates the zone of overlap. **G-I)** Example of cell behavior at an arbitrary boundary in the midbrain. Even though the cell populations are well separated at the 5-somite stage (G), they show a marked overlap after 5 h and at 24 ss (H, I)

For reasons of overview only a subset (leaving out the most dorsal and ventral planes) of the data of the longest movie (12 h) is shown in A-I. The plots are two-dimensional projections along the z-axis (dorsal views) and nuclei sizes are not drawn to scale. Dashed lines show the embryo's midline. A,D,G: Start (5-somite stage) of the movie; B,E,H: Nuclei positions after 5 h (15 ss); C,F,I: End (24 ss) of the movie. Units are in microns in A-I.



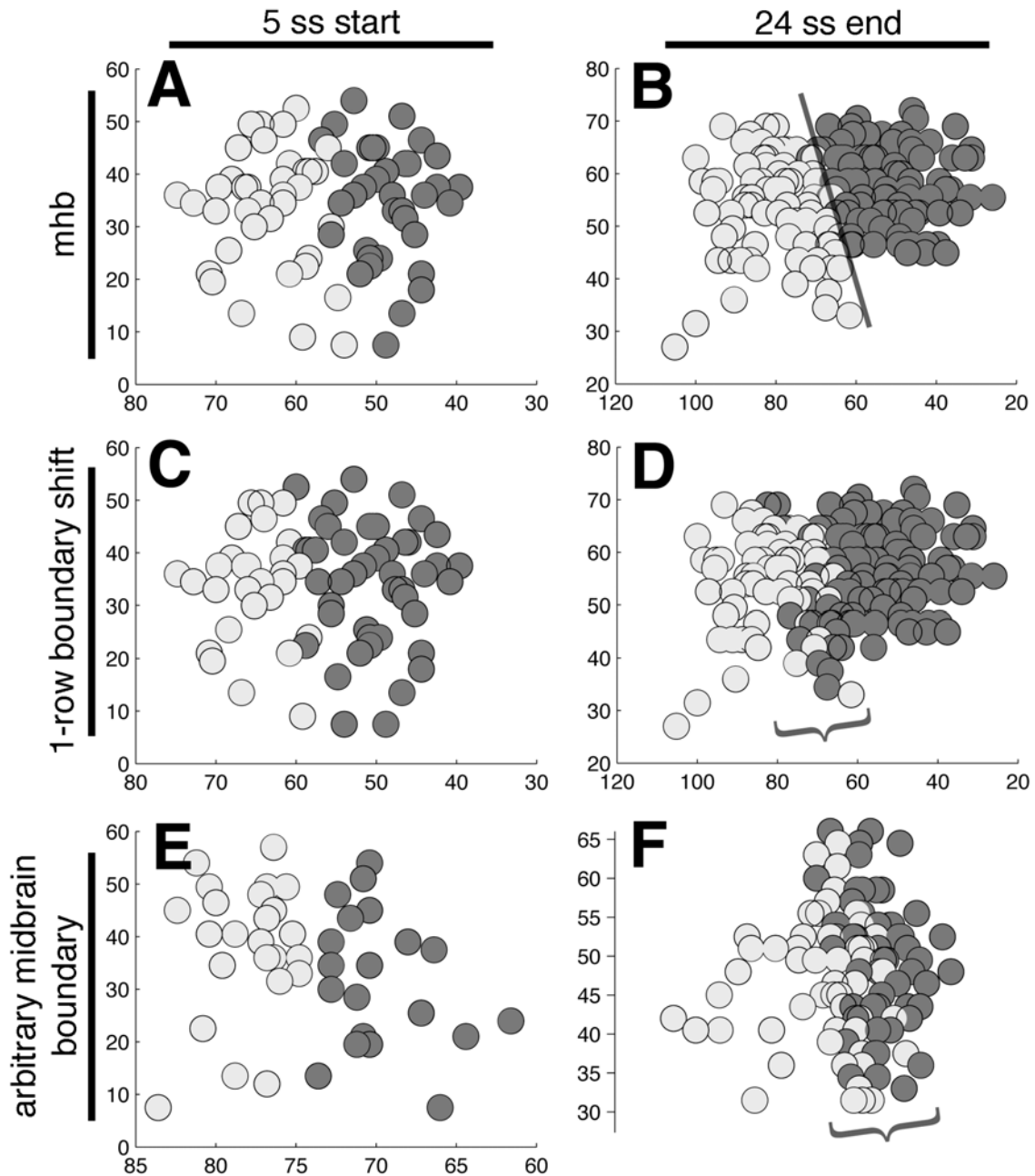


**Figure 11** Summary plots of nuclei positions II

**A,B)** Otx positive and negative nuclei form coherent groups during the time lapse. In the lateral view, this is not always as obvious, compare to fig. 10. **C,D)** Upon shifting the Otx / Otx negative interface artificially by about one cell row at the 5-somite stage (D), the sharp interface of the two cell populations is lost at later stages (E,F). **E,F)** Example of cell behavior at an arbitrary boundary in the midbrain. The plots are two-dimensional projections along the y-axis (lateral views, anterior is to the left). A,D,G: Start (5-somite stage) of the movie; B,E,H: Nuclei positions after 5 h; C,F,I: End (22 hpf) of the movie. Units are in microns.

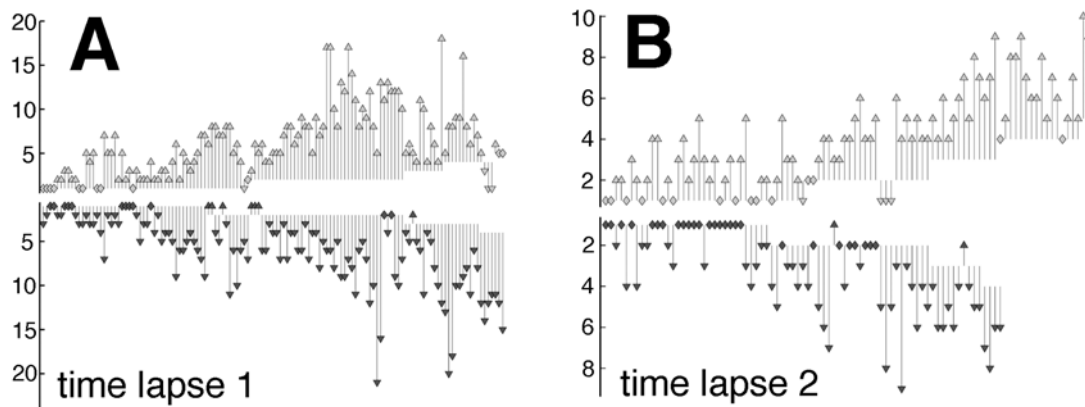


**Figure 12 Cells move away from the Otx interface over time**

**A,B)** Plots showing the relative movement of cells with respect to their common boundary at the mhb from the start to the end of the time lapse. The upper group of arrows represents Otx positive cells, the lower dark one Otx negative cells. Diamonds stand for cells that do not change their row position. **A)** time lapse 1 (12 h); **B)** time lapse 2 (10 h).

In summary, the data presented so far demonstrate clearly that the midbrain-hindbrain boundary in the zebrafish is a lineage restriction boundary from at least the 5-somite stage onwards and is very likely already established during late gastrulation stages.

## Lineage restriction boundary and morphological boundary do not match

Figure 13 (stills from movie C) shows that the morphological indentation does not correspond to the gene expression and lineage restriction boundary. Rather, the Otx interface is always situated a few cell rows anterior to the morphological indentation.

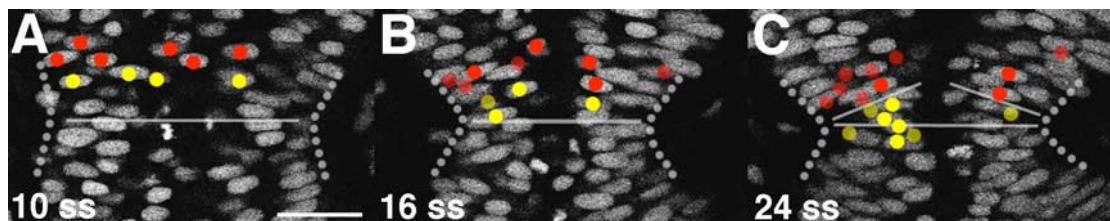


**Figure 13** The morphological boundary does not correspond to the lineage boundary. Red dots mark Otx positive, yellow dots Otx negative cells. The cells marked in B and C are identical to or descendants of the cells in A. The lineage restriction boundary is always found 4-5 cell rows anterior to the morphological constriction, which is marked by the line. Translucent dots mark cells outside the focal plane in B and C. All panels show dorsal views, anterior is to the top. Panels are stills taken from movie C. Scale bar=20 microns

This finding is in agreement with results obtained in the chick embryo (Millet et al., 1996). In this model organism, there is a gap between the posterior border of *otx2* expression and the morphological mhb constriction. The early constriction has therefore been termed “intra-metencephalic”.

Based on my results, I suggest that the earliest morphological indentation in the mhb region of the zebrafish neural tube also resides in the metencephalon and does not separate the mesencephalon from the metencephalon.

## Candidate genes for the lineage restriction mechanism

As the family of Eph receptors and ephrin ligands acts in the hindbrain segmentation process, I analyzed their expression domains in the developing mhb region. Part of this analysis was carried out together with Diana Kadner in a lab practical under my supervision. The following genes were included in the combined analysis:

- ephrin - A2, A3, A5a, A5b, B1, B2a, B2b and B3;
- Eph - A2, A4a, A4b, B2, B4a, B4b;

Most of these genes display very dynamic expression patterns in the brain between 80% epiboly and 24 hpf, which includes the stages during which cell behavior at the mhb was analyzed.

Figure 14 shows the expression domains of some of the most interesting Eph/ephrin pairs at selected stages. *EphB4a/b* (only *EphB4a* expression is shown) are expressed in the midbrain, where their posterior expression border exactly coincides with the posterior expression boundary of *otx2* (fig. 14, A-C). Therefore, the two receptors are expressed anterior to the mhb, exclusively in the midbrain part of the mhb region.

Conversely, *ephrinB2a/b* (only *ephrinB2b* is shown) are expressed in the very anterior hindbrain (fig. 14, D-F), likely abutting *otx2* and *EphB4a/b* expression and therefore exclusively in the hindbrain part of the mhb region. This remains to be verified by double *in-situ* hybridization analysis.

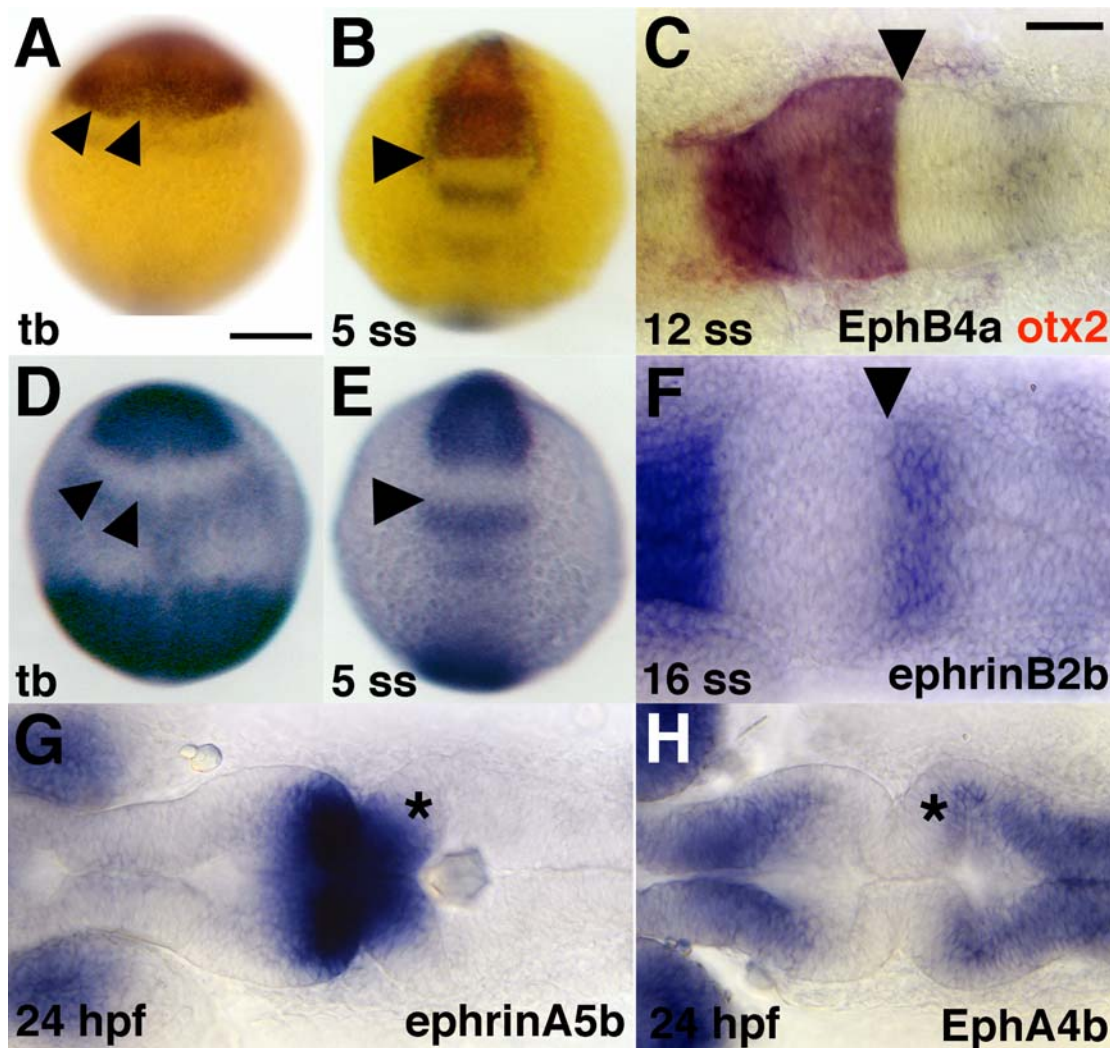


**Figure 14** Expression of Eph receptors and ephrins  
Single (D-H) and double *in-situ* hybridization (A-C) for *Eph* receptors and *ephrins* expressed in the mhb region. **A-C)** *EphB4a* is co-expressed with *otx2* from at least the tailbud (tb) stage onwards. Arrowheads indicate the common posterior expression boundary of *otx2* (red) and *EphB4a* (black). **D-F)** *EphrinB2b* has an expression domain in the anterior hindbrain that seems to be mutually exclusive with *EphB4a* expression. Arrowheads indicate the anterior expression boundary which is located directly at the mhb.

**G, H)** A second pair of ephrin ligand and Eph receptor with a common expression boundary in the middle of the cerebellum at 24 hpf (asterisk). *EphrinA5b* expression spans the mhb while *EphA4b* expression shows a broad gap in the mhb domain. Images D-F were kindly provided by D. Kadner.

All panels show dorsal views, A,B,D,E anterior to the top, C,F,G,H anterior to the left. Scale bars = 50 microns in C (applies to C,F,G,H), 200 microns in A (applies to A,B,D,E).

Based on their expression patterns, these receptor-ligand pairs are good candidates for mediating the lineage restriction at the mhb.

A third interesting pair comprises *ephrinA5a/b* and *EphA4b* (fig. 14 G,H). *EphrinA5a* is expressed in a broad domain spanning the mhb region, while *EphA4b* seems to have a gap in its expression domain of approximately this size. The interface of their expression domains in the middle of the cerebellum at 24 hpf (asterisk in fig. 14 G, H) is of special interest: While analyzing arbitrarily placed control boundaries in the mhb region, I found this region to contain a putative second lineage restriction boundary, as cell mixing was extremely low. Without a precise marker and further studies, the question whether this is a second lineage boundary in the mhb region has to be left open at the moment.

## Embryonic explants

### AMP-PNP blocks curling of explants

The zebrafish yolk cell, like the yolk cell of other teleostean fish embryos, possesses a strongly contractile cortical cytoplasm (Fink, 1988). This cortical cytoplasm contains a dense actomyosin network that becomes activated in response to an elevated  $\text{Ca}^{2+}$  level. Wounding of the yolk cell results in a rapid influx of extracellular  $\text{Ca}^{2+}$ , which quickly activates a massive contractile response of the cortical cytoskeleton (Fink, 1988). When trying to mechanically remove the zebrafish yolk cell, this  $\text{Ca}^{2+}$  induced contractility results in a pronounced curling of the embryo. This curling of body tissues not only impedes imaging of tissue structure and dynamics, it also distorts subsequent morphogenesis of tissue. To block  $\text{Ca}^{2+}$  induced contractility in the yolk cell, I have employed a membrane-impermeable inhibitor of ATPase activity: AMP-PNP (adenosine 5' ( $\beta$ ,  $\gamma$ -imido) triphosphate). This non-hydrolysable membrane-impermeable analog of ATP blocks myosin ATPase activity, and thus 'paralyzes' the contraction of cortical actomyosin networks within the yolk cell.

After yolk cell contractility has been paralyzed, yolk can be easily removed from the yolk cell, without inducing a massive curling of the embryonic axis. Hereafter, I refer to removing yolk from the yolk cell as *deyolking* the embryo. Once the embryo has been deyolked, it can be microdissected into small tissue explants for short-term or long-term culture.

Embryonic explants separated from yolk cells injected with AMP-PNP remain extended in their natural form. The explant can even be slightly flattened against its natural curvature when it is immobilized in agarose or on a plasma clot.

I find that blocking of curling by AMP-PNP injection is not absolutely necessary for very small explants, e. g. the head rudiment with a small portion of the trunk (i.e. the first few somites). In these cases, curvature can be overcome by gently pressing the explant down onto a plasma clot or glass surface (in the case of agarose immobilization). AMP-PNP does not seem to

harm the embryos and explants, since morphogenesis proceeds normally (fig. 15).

## Motional stability of immobilized explants

By cutting away most of the embryo, the problem of motional instability is circumvented. The stickiness of the plasma clot or the gelled agarose prevents explanted tissue from floating or curling, allowing extended imaging without the complications of movement artifacts. Ventral-down mountings are easiest to achieve with the plasma clot, since the remaining yolk cell's EVL/epidermis will stick to the plasma. Both lateral and dorsal down mounts can be done by pushing the explant underneath the clot or by mounting the embryonic explant in low-melting point agarose.

## Normal morphogenesis in cultured explants

To test the viability of the explants, a systematic assay for morphogenetic changes was performed. Embryonic heads were placed into culture at the 18-somite stage (17 hpf) and incubated for 20 h at 28°C (fig. 15). The overall appearance of these explants was normal, tissue integrity was preserved and the explants continued an apparently normal developmental program. In all of these explants (n=12), the following morphogenetic changes could be observed (fig. 15):

The optic cup invaginated and lens formation took place. The neural tube folded at the level of the diencephalon and mhb. This folding was accompanied by the typical growth of the midbrain tectum and the hindbrain cerebellum. Anterior to the telencephalon, the olfactory bulbs separated from the rest of the neuroepithelium. Interestingly, 90% of the explants formed a ventrally located, beating heart during overnight culture (data not shown). Remarkably, a virtually normal mhb formed in the explanted heads. This demonstrates that mhb folding is largely a cell intrinsic process and not dependent on external pressure or ventricle inflation.



Some alterations from normal wild-type development were apparent: In most cases, development of explants seemed to be slowed down. Furthermore, pigmentation was either severely reduced or delayed. The explanted heads had a slightly compressed appearance, which can partly be attributed to the smaller size of the ventricles, especially the first two and the fourth, which were reduced by about one third of their size. This compression was more pronounced when the explants were embedded in agarose.

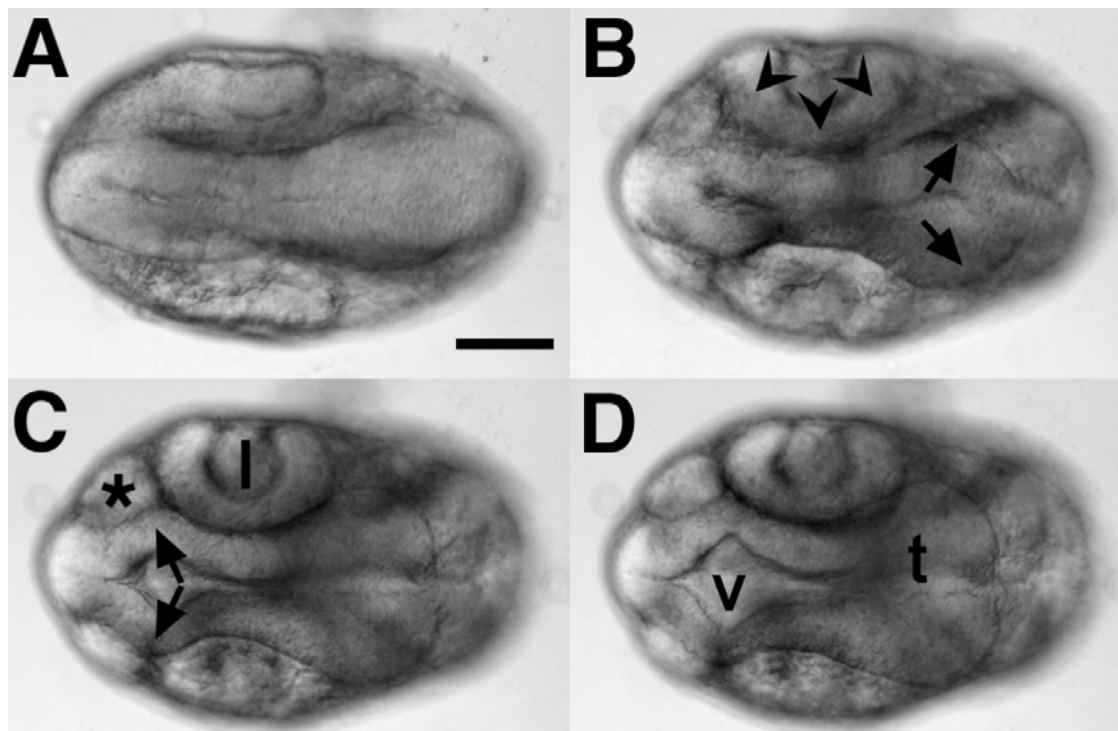


**Figure 15** Stills taken from a movie of a developing head explant. **B-D)** Explant after 7 h, 13 h and 20 h in culture, respectively. **A)** Explant directly after agarose embedding. **B)** Optic cup formation (arrowheads) and tectum growth and folding (arrows) are clearly visible. **C)** The lens (l) has formed, as well as the olfactory bulbs (asterisk marks one). Formation of the third ventricle is ongoing (double arrow). **D)** The third ventricle (v) has formed, as well as the prominent midbrain tectal halves (t). All panels show dorsal views, anterior is to the left. Scale bar=100 microns (applies to A-D).

## Apoptotic cell death is not elevated in cultured explants

Figure 16 illustrates that the number of apoptotic cells is normal or only slightly elevated in explants. To address cell death levels, I performed an acridine orange (AO) staining on explanted heads: Explants (n=7) were made between the 16- and 18-somite stage (17 – 18 hpf) and incubated o/n at 28°C. After 18 hours in culture, medium was exchanged with AO containing (2 µg/ml) L-15 medium and explants were incubated for another 2 h. After washing with medium, incorporated AO was detected under 488 nm excitation. Apart from the massive unspecific accumulation of AO in the remnant of the yolk cell (fig. 16 A,B), only a few cells were positive for acridine orange in the explants. The punctate staining pattern is comparable to that in a wild-type embryo of an equivalent stage (fig. 16 D) and to the results of a recent study of apoptosis in whole embryos (Cole and Ross, 2001). Apoptosis was usually slightly elevated near the side of the cut (fig. 16 B, arrow).

## Gene expression in explanted head rudiments

To address whether explants continue to express important regulatory and patterning genes, I took explants at 18 hpf, incubated them for 20 h and stained for *fgf8* and sonic hedgehog (*shh*) expression by *in-situ* hybridization. Figure 16 shows that both genes are expressed in all their endogenous expression domains. For *fgf8*, *in-situ* signal is detectable in the mhb organizer, the optic stalk, the epiphysis and in the anterior neural plate (fig. 16 E). *Shh* can be detected in the floor plate, the hypothalamus and the ZLI (fig. 16 F). These patterns of gene expression are similar to those in intact embryos (Krauss et al., 1993; Reifers et al., 1998). *Shh* expression in the ZLI normally appears around 24 hpf. Thus, ZLI formation and *shh* expression in this structure occurred after explantation of the head rudiment.

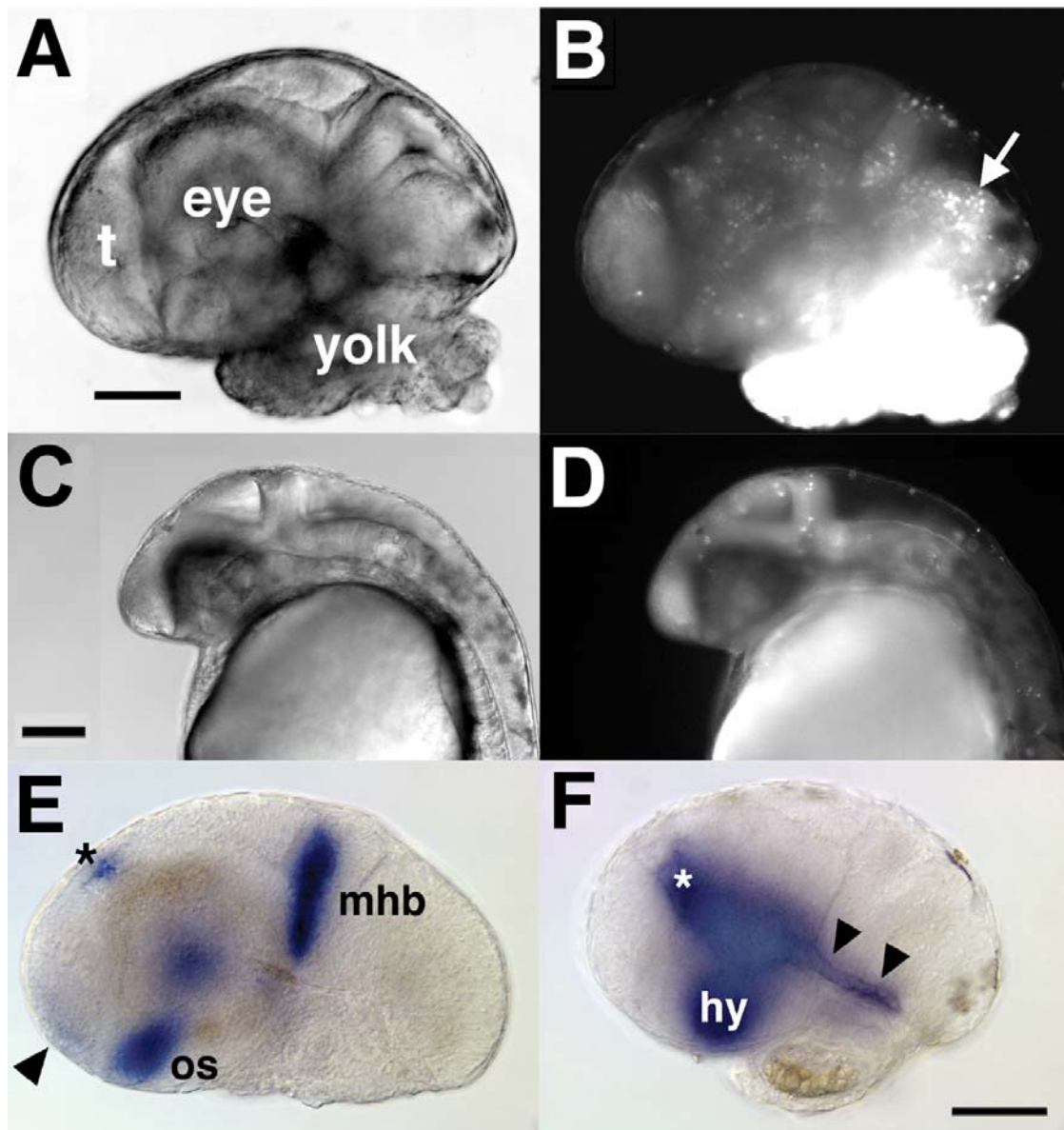


**Figure 16** Apoptosis and gene expression in explants

**A)** DIC image of an agarose-mounted head, explanted at the 16-somite stage, after 20 h of incubation. **B)** The same explant under 488 nm epifluorescence excitation, showing acridine orange (AO) incorporation after 2 h of AO treatment. The remnant yolk has accumulated high amounts of AO, whereas the head shows only slightly elevated, punctate staining. Compare to **C**, **D)** Wild-type embryos at 24 hpf were incubated for 2 h in AO containing medium. Diffuse AO staining in the telencephalon is nonspecific. Scale bars = 100 microns in A (applies to A, B), in C (applies to C, D). **E**, **F)** Head explants stained for *fgf8* (**E**) and *shh* (**F**) expression after 20 h incubation. **E)** Normal expression of *fgf8* is detected in the mhb, the optic stalk (os), the epiphysis (asterisk), and the anterior forebrain (arrowhead). **F)** *Shh* is expressed in the floor plate (arrowheads), the hypothalamus (hy), and the zona limitans intrathalamica (asterisk). Scale bars=100 microns (A applies to A+B, C to C+D, F to E+F).

## Cross-sectional and ventral imaging of embryonic explants

The zebrafish's massive yolk cell makes it very difficult to image ventral organ anlagen in the developing embryo. The bulging yolk cell also reduces working distance when mounting the embryo lateral-side down. Explanting parts of the embryo allows almost any view. High numerical aperture (NA) objectives (e. g. a 40x oil immersion objective with a working distance of less than 100 microns) can be used, because the tissue of interest can be mounted close to the coverslip.

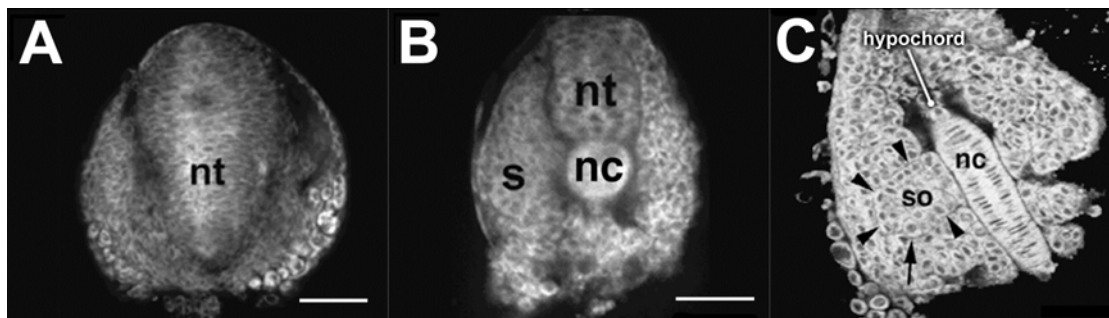


**Figure 17** Cross-sectional and ventral confocal imaging of live explants. The tissues were vitally stained with Bodipy 505/515 before explantation. **A,B**) An 18 hpf embryo; s, somitic mesoderm; nt, neural tube; nc, notochord. (A) Cross-section at the midbrain level, (B) at the trunk level. **C**) Ventral view of an explanted tail rudiment (14-somite stage), mounted ventral down using a plasma clot. The notochord (nc), hypochord and a neighboring somite (so, arrowheads) are clearly visible. An individual somatic mesodermal cell marked (arrow) is in mitotic prophase. Scale bars = 50 microns (B applies to B + C).

Cross-sectional images were produced by transsecting deyolked embryos using a tungsten microneedle. The cut end of the embryo was then placed end-down against the plasma clot.

By reducing the amount of cell material between the objective and the desired plane of focus, high spatial resolution in the epifluorescence confocal image was preserved (fig. 17).

# Discussion

## Lineage restriction at the midbrain-hindbrain boundary

In this work, I have shown that the midbrain and anterior hindbrain of the zebrafish embryo are separated by a lineage restriction boundary. This conclusion is based on the analysis of cell behavior with respect to morphological changes and gene expression patterns in the developing mhb, and on a variety of lineage labeling techniques. Importantly, I carried out lineage analysis with single cell resolution and linked it to the midbrain marker *Otx*.

By imaging the behavior of groups of cells in the mhb region, I have shown that cells on either side of the boundary become separated by a large population of unlabeled cells over time (fig. 7). This region contains the morphological and molecular mhb, as demonstrated by a comparison of *otx2* expression and live morphology (fig. 6). Along with a folding of the a-p axis of the embryo at the mhb, the boundary shifts from perpendicular to tilted with respect to the overall a-p axis of the embryo (fig. 6, 7). I could confirm the finding by Silke Schmitt (Schmitt, 1999) that marker gene expression in the developing mhb follows these morphological changes (fig. 6).

Dil bulk labeling of cells in the vicinity of the mhb mostly yielded clones that were restricted to one side of the mhb (fig. 8).

Single cell labeling by iontophoretic injection at late gastrulation stages showed that clones were predominantly restricted to one side of the mhb (fig. 8). These findings have to be reconciled with the arrangement of neuroepithelial cells in a pseudo-stratified epithelium, where they only have few degrees of freedom (Papan, 1994). The data summarized in table 1 demonstrate that clones derived from single cell injections display a relatively limited growth and spreading along the a-p axis during the period of strong morphological changes at the mhb.

In the light of these findings, I decided to image and follow all cells near the molecular boundary (as marked by *Otx* antibody staining) during the folding

process of the mhb region. The detailed analysis of the movement of hundreds of individual nuclei (table 2 and fig. 9-11) demonstrates clearly that cells do not mix between an *Otx* positive and an *Otx* negative population at least from the 5-somite stage onwards. By comparing cell position at the beginning and end of the imaging period, I can corroborate the finding derived from spinning disc time lapse microscopy, that cells move away from the molecular and morphological boundary (fig. 10-12), but virtually never across it. Notably, the earliest morphological indentation in the mhb region does not correspond to the molecular and lineage boundary (fig. 13).

In summary, these data proof that a compartment boundary separates the dorsal midbrain and hindbrain in the zebrafish embryo. As this region contains an organizer, I want to briefly discuss mhb organizer function.

### The mhb organizer

The midbrain-hindbrain boundary organizer is the prime example of a neuroepithelial secondary organizer and has therefore been subject to intensive studies. Several reviews about the isthmic organizer have been published (Puelles et al., 1996; Joyner et al., 2000; Rhinn and Brand, 2001; Wurst and Bally-Cuif, 2001; Raible, 2004) and a complete recapitulation of mhb formation and function is beyond the scope of this thesis, therefore, I will only discuss some early aspects of mhb organizer development.

One of the first crucial steps in organizer formation is a subdivision of the neural plate into *otx*- and *gbx*-expressing territories. The interface of these two transcription factors then determines the position of the mhb organizer (Millet et al., 1996; Wassarman et al., 1997; Broccoli et al., 1999; Hidalgo-Sanchez et al., 1999b; Martinez et al., 1999; Millet et al., 1999; Garda et al., 2001; Rhinn et al., 2003). In the zebrafish, *otx* and *gbx* expression slightly overlap during early gastrulation stages, while they abut each other at 80% epiboly (Rhinn et al., 2003). Subsequently, at this interface, at least three signaling pathways become activated independently of each other, marked by the expression of *wnt1*, *pax2.1* and *fgf8*. During a maintenance phase, these factors soon become interdependent (Lun and Brand, 1998; Reifers et al., 1998). Consequently, disrupting any of the three genes will lead to a

breakdown of organizer function (Bally-Cuif et al., 1995a; Brand et al., 1996; Danielian and McMahon, 1996; Favor et al., 1996; Lun and Brand, 1998; Meyers et al., 1998; Pfeffer et al., 1998; Reifers et al., 1998).

Given their potency as organizing molecules, both *fgf8* and *wnt1* expression have to be carefully controlled in the embryo. This control has to be exerted on multiple levels, the most basal ones being when and where onset of expression is allowed. *Fgf8* expression is found exclusively in the anterior *gbx* domain, while *wnt1* expression becomes refined to a small stripe in the posterior *otx* domain. For an ordered onset and maintenance of sharply defined organizing cell populations, lineage restriction between neighboring compartments that control the expression of such organizing molecules appears to be a crucial mechanism. This link between organizers and lineage boundaries has been discovered in the fly (Crick and Lawrence, 1975; Dahmann and Basler, 1999) and is also found in vertebrate limb formation (Kimmel et al., 2000).

Based mainly on the observations in chick, it was suggested (Wurst and Bally-Cuif, 2001) that the midbrain and hindbrain are not separated by a lineage restriction boundary. This would require rather elaborate mechanisms based on plasticity to maintain sharp gene expression domains in the developing mhb region. The findings presented in this thesis rather indicate that there is a very early separation of cell lineage at the mhb, possibly already during the neural plate stage, towards the end of gastrulation. This would allow a clear spatial control over gene expression domains at the mhb.

#### Lineage restriction at the mhb - other model organisms

Lineage restriction at the mhb has been addressed in other vertebrate model systems with conflicting results. A recent study in mouse (Zervas et al., 2004) suggests the existence of several lineage restriction boundaries in the mhb region, one of them situated at the dorsal mesencephalon-metencephalon interface. The authors have made use of a genetic labeling approach, crossing mice strain carrying a Tamoxifen inducible Cre recombinase, controlled by the endogenous *wn1* promoter, to a lacZ driver line. This method allows genetic labeling of a large number of cells at a chosen time point and

the analysis of their distribution at later stages. However, this approach can only indirectly address cell movement, as cell behavior between labeling and readout is not visualized and a cellular resolution is not obtained.

My approach of directly visualizing cell movement on the single cell level allowed me to address the behavior of cells on both sides of the mhb, clearly showing that there is no mixing between the two cell populations.

Zervas et al. consistently find a small number of lacZ positive cells in the cerebellum, independent of the time of labeling. As discussed by the authors, *wnt1* is initially expressed throughout the midbrain and overlaps slightly with *gbx* expression in the anterior hindbrain (Bally-Cuif et al., 1995a; Millet et al., 1996; Hidalgo-Sanchez et al., 1999a; Matsunaga et al., 2002), thus effectively spanning the midbrain-hindbrain border. The choice of this driver line can provide an explanation for the observed violation of lineage restriction: Because Cre recombinase is constantly produced in Wnt1 positive cells, residual Cre may remain stable and catalyze labeling of cells that, at later stages, no longer express Wnt1. Upon Tamoxifen-dependent Cre induction, lacZ would be expressed in these cells outside the endogenous Wnt1 domain. In the absence of directly observing cell movement at the cellular level, it is therefore difficult to ascertain lineage restriction in this system.

By following the movement of individual cells within the mhb region, I have detected only two cells (out of 551 within a few cell diameters of the boundary) that did not respect the lineage restriction boundary (table 2). Two Otx negative cells were traced backwards and derived from the same founder cell within the Otx positive domain at the start of the time lapse. There are at least two possible explanations for this exception to the rule: (i) I may have wrongly assigned these cells or mistracked them repeatedly. However, given my overall high accuracy of tracking, I consider this unlikely. (ii) More likely, the restriction mechanism may be somewhat leaky, as reported for rhombomeres (Birgbauer and Fraser, 1994). Escapers would require some level of plasticity in gene expression to adopt the target tissue's fate.

Two recent reports in the chick claim to see a contribution of a distinct cell population in the roof plate of the mhb to both midbrain and hindbrain roof plate structures (Alexandre and Wassef, 2003; Louvi et al., 2003). This cell



population would therefore not respect a cell lineage restriction between the midbrain and hindbrain. These cell movement analyses, using Dil labeling or the quail-chick grafting system, do not reach single cell resolution. External application of Dil to a (however small) group of cells will not yield a sufficient resolution to directly test for a lineage restriction mechanism. This is certainly also true for the quail-chick grafting system, which, in addition, has other known drawbacks, namely proliferation and cell adhesion differences between quail and chick cells (Senut and Alvarado-Mallart, 1986; Martinez and Alvarado-Mallart, 1989).

In general, the situation in chick is not as clear as in other organisms, with a recent study rejecting a lineage restriction at the mhb (Jungbluth et al., 2001). As other groups in principal support a lineage restriction mechanism at the chick mhb (Millet et al., 1996; Alexandre and Wassef, 2003; Louvi et al., 2003), with the above discussed possible exception of the roof plate, further investigations seem necessary to clarify the situation.

In this study, I have also detected very dorsally located cells that seemed to violate the lineage restriction boundary (table 2). All of these either left the neuroepithelium (18/22) during the imaged time period or moved over unusually large distances (4/22), classifying them as putative neural crest cells. Therefore, I argue that there is no contribution of midbrain cells to anterior hindbrain structures in the zebrafish. In the absence of recording the long-term fate of putative neural crest cells I cannot exclude that a small dorsal population of cells ignores the lineage boundary.

Clonal dispersion in the brain after single cell injections has been addressed in another fish species, Medaka (*Oryzias latipes*) (Hirose et al., 2004). The authors combined data derived from 150 single cell injections in a computer-based model of the developing Medaka embryo. Interestingly, they claim to see a simultaneous onset of lineage restriction between all examined brain regions (telencephalon, diencephalon, mesencephalon and metencephalon) at the transition from developmental stage 16+ to 17, which corresponds approximately to the tailbud stage in zebrafish. Although starting from single injected cells, the authors do not establish a direct link to genetic markers,

therefore their findings cannot be taken as a proof for the existence of lineage boundaries in the Medaka brain.

### Concluding remarks

Combining our findings with those in mouse (Zervas et al., 2004), it is becoming clear that the mhb separates two neuromeres, thereby extending the neuromeric model of brain formation to this part of the vertebrate neural tube.

It is as yet unclear whether the anterior neural tube is compartmentalized in general, similar to the rhombencephalon. Rather, lineage restriction boundaries have so far only been identified framing the zona limitans intrathalamica (ZLI) (Larsen et al., 2001), at the diencephalon-mesencephalon (di-mes) border (Larsen et al., 2001; Zervas et al., 2004) and at the mhb (this study and (Zervas et al., 2004)). Including the putative r4-organizer (Maves et al., 2002; Walshe et al., 2002), a picture emerges where cell populations secreting organizing molecules (Fgf8/Wnt1 at the mhb, Fgf8/Fgf3 in rhombomere 4 and Shh at the ZLI) are flanked by neuromere boundaries. The reverse conclusion can apparently not be drawn, as several rhombomere boundaries and the di-mes border are not known to be associated with organizers.

I believe that further studies addressing the relationship between organizing cell populations and lineage restriction boundaries will contribute substantially to our understanding of early brain development.

## Embryonic explants

Motional stability is critical for successful 3D and 4D imaging of live embryonic tissues. Cells and tissues of interest must be maintained within the field of view during the course of image acquisition, without having the specimen roll, translocate, vibrate, deform, or lose viability.

The thin plasma clot technique offers a versatile means of securing deyolked zebrafish embryos, as well as embryonic explants extirpated from them. Utilizing the non-hydrolysable ATP analog, AMP-PNP, is a new way of deyolking zebrafish embryos, that avoids unwanted yolk cell contractility.

The immobilized explants provide an extended field of view for immediate imaging, as well as a stable mounting for novel views of the embryo, such as ventral, lateral or even cross-sectional.

Embryonic explants have long provided unique opportunities for developmental biologists, to examine the structure and behavior of embryonic cells within their native tissue environments. Nearly a century ago, cultured explants of embryonic tissues were first used to examine the outgrowth and motile behavior of individual neurons (Harrison, 1910; Harrison, 1914). Since that time, explanted embryonic tissues have been widely used to examine patterning, morphogenesis (Schechtman, 1942; Trinkaus and Drake, 1956; Wilson et al., 1989; Wilson and Keller, 1991; O'Rourke et al., 1992; O'Rourke et al., 1995) and the electrophysiology of developing tissues (Gähwiler, 1981; Gähwiler, 1984a; Gähwiler, 1984b).

Short-term culturing of deyolked fish embryos has been performed numerous times by others (Oppenheimer, 1936; Tung, 1944; Tung and Chang, 1945; Trinkaus and Drake, 1956; Bozhkova VG, 1994; Simon, 1995; Grinblat, 1999; te Kronnie G, 2000). None of these studies employed immobilization media for time-lapse imaging or analyzed the development of complex tissue structures in intermediate stages of development after explantation. Rather, they either focused on blastula- to gastrula-stage explants or on very late embryonic explants, when derived morphological structures had already formed. Blastula- to gastrula-stage explants were performed with a bias on

the analysis of patterning and induction. In fact, survival times for very early explants were on the several hours scale only (Grinblat, 1999).

I have found that tissues develop fairly normally for up to 24 h without medium exchange in cultured explants that are either immobilized in agarose or on a plasma clot. One noticeable difference is the reduction or lack of pigmentation in cultured explants compared to intact embryos. I speculate that the lack of pigment cell differentiation in the embryonic explants might be connected with the loss of a growth factor normally carried through blood circulation. Reduced ventricle expansion is often observed in immobilized head explants. It is possible that cerebrospinal fluid may be leaking from the cut end of the end of the developing head explant. In addition, when head rudiments are completely gelled within agarose, the mechanical pressure of immobilization may inhibit ventricle expansion. This problem should be obviated when head rudiments are immobilized on the surface of a plasma clot.

In teleostean fish embryo, the fragility of the yolk cell has hampered the development and application of certain experimental embryological techniques, such as organ rudiment transplantation or inversion of whole tissue blocks. These techniques have long been utilized in amphibian and avian embryos (Spemann, 1924; Le Douarin, 1973; Stern, 1999; Alvarado-Mallart, 2000; Packard et al., 2000). The ability to mount and culture a deyolked zebrafish embryo using thin plasma clot immobilization, may improve the ability to perform tissue transplantation and other micromanipulations in zebrafish embryos.

Cultured embryonic explants also offer a number of potential other applications. By placing deyolked embryos in culture media, it may be possible to nurse mutant embryos through critical periods in their development, when early acting embryonic lethal genes would normally result in the death of the embryo. This could allow downstream effects of these genes to be studied at later time points of development. It should also be possible to follow the behavior of fluorescently labeled pathogens in immobilized cultured explants, as has recently been demonstrated in the intact zebrafish embryos and larvae (Davis et al., 2002)

By isolating embryonic tissue parts, the effects of specific drugs or small molecules can be studied without affecting the rest of the body and thereby producing artifacts or unwanted side effects.

Cultured cross-sectional slices of embryos may also provide unique opportunities for studying organogenesis and histodifferentiation in developing zebrafish tissues.

# Movie descriptions

## Movie A: mhb formation

The movie shows a dorsal view of the mhb region of a developing zebrafish embryo, anterior is to the left. The developmental stage is indicated in the bottom left corner in either somites or hpf.

The first indentation (marked by arrowheads) matures into the deep invagination that separates the midbrain from the hindbrain. The dotted line indicates the folding of the mhb region, two lines show the approximate position of the molecular (*otx/gbx* interface) boundary.

cb – cerebellum; hb – hindbrain; mb – midbrain; 3rd v. and 4th v. – third and fourth ventricle

## Movie B: cell behavior during mhb formation

Movie B is assembled from a spinning disc confocal time lapse, showing the developing mhb region of a living zebrafish embryo that contains GFP expressing cells. Shown is a dorsal view, anterior is to the left. The movie starts at about the 10-somite stage and follows mhb development up to about 30 hpf. Red dots mark future midbrain cells, yellow dots future hindbrain cell, black arrowheads mark the boundary. During the movie, the formation of the third ventricle is indicated by white dots. Black dotted lines mark the mhb indentation at later stages.

Two cell populations on either side of the mhb become separated by a gap of unlabeled cells. No mixing between the cell populations can be observed. Despite strong morphological changes, movement of individual cells seems relatively restricted

Movie C: following individual cells

This movie is assembled from time lapse three (table 2), starting at the 10-somite stage and ending at the 24-somite stage. A stripe of nuclei directly at the boundary is marked by red (Otx positive) and yellow (Otx negative) dots. The nuclei are then followed throughout the whole sequence. As the movie is restricted to one focal plane, several of the nuclei disappear from view. At the end of the movie, these are marked by translucent dots in their correct xy position.

As the embryo develops, initially neighboring nuclei become separated and move several cell rows away from each other. Despite this movement, nuclei remain within their respective groups and are separated by a clear boundary (grey line at the end of the movie).

Many cells can be seen to divide at the midline. Two of these cells are marked by an arrow before and by two arrowheads after division. The first division gives rise to daughter cells in both halves of the neural tube, the second division is oriented in an a-p direction. Here, right after division, one daughter cell is located slightly within the Otx positive domain, but reintegrates into the Otx negative cell population.

Grey dotted lines mark the outline of the neural plate.

## References

- Ahlborn, F.** (1883). Untersuchungen über das Gehirn der Petromyzonten. *Z. Wiss. Zool.* **39**, 191-294.
- Alexandre, P. and Wassef, M.** (2003). The isthmic organizer links anteroposterior and dorsoventral patterning in the mid/hindbrain by generating roof plate structures. *Development* **130**, 5331-8.
- Alvarado-Mallart, R. M.** (2000). The chick/quail transplantation model to study central nervous system development. *Prog Brain Res* **127**, 67-98.
- Baer, K. E. v.** (1828). Über die Entwicklungsgeschichte der Thiere. *Königsberg* **1-3**.
- Bally-Cuif, L., Cholley, B. and Wassef, M.** (1995a). Involvement of *Wnt-1* in the formation of the mes/metencephalic boundary. *Mech. Dev.* **53**, 23-34.
- Bally-Cuif, L., Gulisano, M., Broccoli, V. and Boncinelli, E.** (1995b). *c-otx2* is expressed in two different phases of gastrulation and is sensitive to retinoic acid treatment in chick embryo. *Mech Dev* **49**, 49-63.
- Bergquist, H. and Kallen, B.** (1953). Studies on the topography of the migration areas in the vertebrate brain. *Acta Anat (Basel)* **17**, 353-69.
- Bergquist, H. and Kallen, B.** (1954). Notes on the early histogenesis and morphogenesis of the central nervous system in vertebrates. *J Comp Neurol* **100**, 627-59.
- Birgbauer, E. and Fraser, S. E.** (1994). Violation of cell lineage restriction compartments in the chick hindbrain. *Development* **120**, 1347-56.
- Bozhkova VG, t. K. G., Timmermans LPM.** (1994). Mesoderm differentiation in explants of carp embryos. *Roux's Archives in Developmental Biology* **204**, 20-29.
- Brand, M. and Granato, M.** (2000). Keeping and raising zebrafish. In *Zebrafish: A Practical Approach*, (ed. C. Nüsslein-Volhard and S. Schulte-Merker), pp. in press. Oxford: IRL Press.
- Brand, M., Heisenberg, C.-P., Jiang, Y.-J., Beuchle, D., Lun, K., van Eeden, F. J. M., Furutani-Seiki, M., Granato, M., Haffter, P., Hammerschmidt, M. et al.** (1996). Mutations in zebrafish genes affecting the formation of the boundary between midbrain and hindbrain. *Development* **123**, 179-190.
- Brennan, C., Monschau, B., Lindberg, R., Guthrie, B., Drescher, U., Bonhoeffer, F. and Holder, N.** (1997). Two Eph receptor tyrosine kinase ligands control axon growth and may be involved in the creation of the retinotectal map in the zebrafish. *Development* **124**, 655-64.
- Broccoli, V., Boncinelli, E. and Wurst, W.** (1999). The caudal limit of *Otx2* expression positions the isthmic organizer. *Nature* **401**, 164-168.
- Chan, J., Mably, J. D., Serluca, F. C., Chen, J. N., Goldstein, N. B., Thomas, M. C., Cleary, J. A., Brennan, C., Fishman, M. C. and Roberts, T.**



- M.** (2001). Morphogenesis of prechordal plate and notochord requires intact Eph/ephrin B signaling. *Dev Biol* **234**, 470-82.
- Chandrasekhar, A., Moens, C. B., Warren, J. T., Jr., Kimmel, C. B. and Kuwada, J. Y.** (1997). Development of branchiomotor neurons in zebrafish. *Development* **124**, 2633-44.
- Chi, C. L., Martinez, S., Wurst, W. and Martin, G. R.** (2003). The isthmic organizer signal FGF8 is required for cell survival in the prospective midbrain and cerebellum. *Development* **130**, 2633-44.
- Colas, J. F. and Schoenwolf, G. C.** (2001). Towards a cellular and molecular understanding of neurulation. *Dev Dyn* **221**, 117-45.
- Cole, L. K. and Ross, L. S.** (2001). Apoptosis in the developing zebrafish embryo. *Dev Biol* **240**, 123-42.
- Concha, M. L. and Adams, R. J.** (1998). Oriented cell divisions and cellular morphogenesis in the zebrafish gastrula and neurula: a time-lapse analysis. *Development* **125**, 983-94.
- Cooke, J., Moens, C., Roth, L., Durbin, L., Shiomi, K., Brennan, C., Kimmel, C., Wilson, S. and Holder, N.** (2001). Eph signalling functions downstream of Val to regulate cell sorting and boundary formation in the caudal hindbrain. *Development* **128**, 571-80.
- Cooper, M. S., D'Amico, L. A. and Henry, C. A.** (1999). Analyzing morphogenetic cell behaviors in vitally stained zebrafish embryos. *Methods Mol Biol* **122**, 185-204.
- Crick, F. H. C. and Lawrence, P. A.** (1975). Compartments and Polyclones in Insect Development. *Science* **189**, 340-347.
- Crossley, P. H. and Martin, G. R.** (1995). The mouse Fgf8 gene encodes a family of polypeptides and is expressed in regions that direct outgrowth and patterning in the developing embryo. *Development* **121**, 439-451.
- Crossley, P. H., Martinez, S. and Martin, G. R.** (1996). Midbrain development induced by FGF8 in the chick embryo. *Nature* **380**, 66-8.
- Dahmann, C. and Basler, K.** (1999). Compartment boundaries: at the edge of development. *Trends Genet* **15**, 320-6.
- Danielian, P. S. and McMahon, A. P.** (1996). *Engrailed-1* as a target of the *Wnt-1* signalling pathway in vertebrate midbrain development. *Nature* **383**, 332-334.
- Davis, J. M., Clay, H., Lewis, J. L., Ghori, N., Herbomel, P. and Ramakrishnan, L.** (2002). Real-time visualization of mycobacterium-macrophage interactions leading to initiation of granuloma formation in zebrafish embryos. *Immunity* **17**, 693-702.
- Denk, W., Strickler, J. H. and Webb, W. W.** (1990). Two-photon laser scanning fluorescence microscopy. *Science* **248**, 73-6.
- Durbin, L., Brennan, C., Shiomi, K., Cooke, J., Barrios, A., Shanmugalingam, S., Guthrie, B., Lindberg, R. and Holder, N.** (1998). Eph signaling is required for segmentation and differentiation of the somites. *Genes Dev* **12**, 3096-109.

- Echevarria, D., Vieira, C., Gimeno, L. and Martinez, S.** (2003). Neuroepithelial secondary organizers and cell fate specification in the developing brain. *Brain Res Brain Res Rev* **43**, 179-91.
- Ettensohn, C. A.** (1985). Mechanisms of epithelial invagination. *Q Rev Biol* **60**, 289-307.
- Favor, J., Sandulache, R., Neuhäuser-Klaus, A., Pretsch, W., Chatterjee, B., Senft, E., Wurst, W., Blanquet, V., Grimes, P., Spörle, R. et al.** (1996). The mouse Pax21Neu mutation is identical to a human PAX2 mutation in a family with renal-coloboma syndrome and results in developmental defects of the brain, ear, eye and kidney. *PNAS* **93**, 13870-13875.
- Fink, R. D. T., J. P.** (1988). Fundulus Deep Cells: Directional Migration in Response to Epithelial Wounding. *Dev Biol* **129**, 179-190.
- Fraser, S., Keynes, R. and Lumsden, A.** (1990). Segmentation in the chick embryo hindbrain is defined by cell lineage restrictions. *Nature* **344**, 431-435.
- Fraser, S. E.** (1996). Iontophoretic Dye Labeling of Embryonic Cells. *Methods in Cell Biology* **51**, 147-160.
- Gähwiler, B. H.** (1981). Organotypic monolayer cultures of nervous tissue. *J Neurosci Meth* **4**, 329-342.
- Gähwiler, B. H.** (1984a). Guidance of acetylcholinesterase-containing fibres by target tissue in co-cultured brain slices. *Neuroscience* **13**, 681-689.
- Gähwiler, B. H.** (1984b). Slice cultures of cerebellar, hippocampal and hypothalamic tissue. *Experientia* **40**, 235-243.
- Garcia-Bellido, A., Ripoll, P. and Morata, G.** (1973). Developmental compartmentalisation of the wing disk of *Drosophila*. *Nat New Biol* **245**, 251-3.
- Garda, A. L., Echevarria, D. and Martinez, S.** (2001). Neuroepithelial co-expression of Gbx2 and Otx2 precedes Fgf8 expression in the isthmic organizer. *Mech Dev* **101**, 111-8.
- Geldmacher-Voss, B., Reugels, A. M., Pauls, S. and Campos-Ortega, J. A.** (2003). A 90-degree rotation of the mitotic spindle changes the orientation of mitoses of zebrafish neuroepithelial cells. *Development* **130**, 3767-80.
- Gilland, E. and Baker, R.** (1993). Conservation of neuroepithelial and mesodermal segments in the embryonic vertebrate head. *Acta Anat (Basel)* **148**, 110-23.
- Grinblat, e. a.** (1999). Analysis of Zebrafish Development Using Explant Culture Assays. *Methods Cell Biol* **59**, 127-156.
- Guthrie, S., Butcher, M. and Lumsden, A.** (1991). Patterns of cell division and interkinetic nuclear migration in the chick embryo hindbrain. *J Neurobiol* **22**, 742-54.
- Guthrie, S., Prince, V. and Lumsden, A.** (1993). Selective dispersal of avian rhombomere cells in orthotopic and heterotopic grafts. *Development* **118**, 527-38.

- Halloran, M. C. and Berndt, J. D.** (2003). Current progress in neural crest cell motility and migration and future prospects for the zebrafish model system. *Dev Dyn* **228**, 497-513.
- Harrison, R. G.** (1910). The outgrowth of the nerve fiber as a mode of protoplasmic movement. *J Exp Zool* **9**, 787-846.
- Harrison, R. G.** (1914). The reaction of embryonic cells to solid structure. *J Exp Zool* **17**, 521-544.
- Hidalgo-Sanchez, M., Millet, S., Simeone, A. and Alvarado-Mallart, R. M.** (1999a). Comparative analysis of Otx2, Gbx2, Pax2, Fgf8 and Wnt1 gene expressions during the formation of the chick midbrain/hindbrain domain. *Mech Dev* **81**, 175-8.
- Hidalgo-Sanchez, M., Simeone, A. and Alvarado-Mallart, R. M.** (1999b). Fgf8 and Gbx2 induction concomitant with Otx2 repression is correlated with midbrain-hindbrain fate of caudal prosencephalon. *Development* **126**, 3191-203.
- Hirose, Y., Varga, Z. M., Kondoh, H. and Furutani-Seiki, M.** (2004). Single cell lineage and regionalization of cell populations during Medaka neurulation. *Development* **131**, 2553-63.
- Holder, N. and Klein, R.** (1999). Eph receptors and ephrins: effectors of morphogenesis. *Development* **126**, 2033-44.
- Houart, C., Westerfield, M. and Wilson, S. W.** (1998). A small population of anterior cells patterns the forebrain during zebrafish gastrulation. *Nature* **391**, 788-792.
- Ingham, P.** (1988). The molecular genetics of embryonic pattern formation in *Drosophila*. *Nature* **335**, 25-34.
- Jaszai, J., Reifers, F., Picker, A., Langenberg, T. and Brand, M.** (2003). Isthmus-to-midbrain transformation in the absence of midbrain-hindbrain organizer activity. *Development* **130**, 6611-23.
- Joyner, A. L., Liu, A. and Millet, S.** (2000). Otx2, Gbx2 and Fgf8 interact to position and maintain a mid-hindbrain organizer. *Curr Opin Cell Biol* **12**, 736-41.
- Jungbluth, S., Larsen, C., Wizenmann, A. and Lumsden, A.** (2001). Cell mixing between the embryonic midbrain and hindbrain. *Curr Biol* **11**, 204-7.
- Källén, B.** (1962). Mitotic patterning in the central nervous system of chick embryos; studied by a colchicine method. *Z. Anat. Entw.-Gesch.* **123**, 309-319.
- Kelly, G. M., Lai, C. J. and Moon, R. T.** (1993). Expression of wnt10a in the central nervous system of developing zebrafish. *Developmental Biology* **158**, 113-21.
- Keynes, R., Cook, G., Davies, J., Lumsden, A., Norris, W. and Stern, C.** (1990). Segmentation and the development of the vertebrate nervous system. *J Physiol (Paris)* **84**, 27-32.

- Kimmel, C. B., Ballard, W. W., Kimmel, S. R., Ullmann, B. and Schilling, T. F.** (1995). Stages of embryonic development of the zebrafish. *Dev. Dyn.* **203**, 253-310.
- Kimmel, R. A., Turnbull, D. H., Blanquet, V., Wurst, W., Loomis, C. A. and Joyner, A. L.** (2000). Two lineage boundaries coordinate vertebrate apical ectodermal ridge formation. *Genes Dev* **14**, 1377-89.
- Krauss, S., Concordet, J. P. and Ingham, P. W.** (1993). A functionally conserved homolog of the *Drosophila* segment polarity gene *hh* is expressed in tissues with polarizing activity in zebrafish embryos. *Cell* **75**, 1431-44.
- Kullander, K. and Klein, R.** (2002). Mechanisms and functions of Eph and ephrin signalling. *Nat Rev Mol Cell Biol* **3**, 475-86.
- Langenberg, T.** (2000). *In vivo* time lapse Analyse von Zellverhalten und Morphogenese bei der Entwicklung der Mittel-Hinterhirn-Grenzregion im Zebrafisch, *Danio rerio*. *Diploma Thesis*.
- Larsen, C. W., Zeltser, L. M. and Lumsden, A.** (2001). Boundary formation and compartition in the avian diencephalon. *J Neurosci* **21**, 4699-711.
- Lawrence, P. A. and Morata, G.** (1976). Compartments in the Wing of *Drosophila*: A Study of the engrailed Gene. *Developmental Biology* **50**, 321-337.
- Layer, P. G. and Alber, R.** (1990). Patterning of chick brain vesicles as revealed by peanut agglutinin and cholinesterases. *Development* **109**, 613-24.
- Le Douarin, N.** (1973). A biological cell labeling technique and its use in experimental embryology. *Dev Biol* **30**, 217-22.
- Lewis, E. B.** (1978). A gene complex controlling segmentation in *Drosophila*. *Nature* **276**, 565-570.
- Locy, W. A. C.** (1895). Contribution to the structure and development of the vertebrate brain. *J. Morph.* **4**, 35-56.
- Louvi, A., Alexandre, P., Metin, C., Wurst, W. and Wassef, M.** (2003). The isthmic neuroepithelium is essential for cerebellar midline fusion. *Development* **130**, 5319-30.
- Lowery, L. A., Sive, H.** (2004). Strategies of vertebrate neurulation and a re-evaluation of teleost neural tube formation. *Mech Dev* **in press**.
- Lumsden, A. and Keynes, R.** (1989). Segmental patterns of neuronal development in the chick hindbrain. *Nature* **337**, 424-428.
- Lumsden, A. and Krumlauf, R.** (1996). Patterning the vertebrate neuraxis. *Science* **274**, 1109-1115.
- Lun, K. and Brand, M.** (1998). A series of no isthmus (*noi*) alleles of the zebrafish *pax2.1* gene reveals multiple signaling events in development of the midbrain-hindbrain boundary. *Development* **125**, 3049-3062.
- Mangold, O.** (1933). Über die Induktionsfähigkeit der verschiedenen Bezirke der Neurula von Urodelen. *Naturwissenschaften* **21**.

- Marin, F. and Puelles, L.** (1994). Patterning of the embryonic avian midbrain after experimental inversions: a polarizing activity from the isthmus. *Dev. Biol.* **163**, 19-37.
- Martinez, S. and Alvarado-Mallart, R. M.** (1989). Rostral Cerebellum Originates from the Caudal Portion of the So-Called 'Mesencephalic' Vesicle: A Study Using Chick/Quail Chimeras. *Eur J Neurosci* **1**, 549-560.
- Martinez, S., Crossley, P. H., Cobos, I., Rubenstein, J. L. and Martin, G. R.** (1999). FGF8 induces formation of an ectopic isthmic organizer and isthmo-cerebellar development via a repressive effect on Otx2 expression. *Development* **126**, 1189-200.
- Martinez, S., Wassef, M. and Alvarado-Mallart, R. M.** (1991). Induction of a mesencephalic phenotype in the 2-day-old chick prosencephalon is preceded by the early expression of the homeobox gene *en*. *Neuron* **6**, 971-981.
- Matsunaga, E., Katahira, T. and Nakamura, H.** (2002). Role of Lmx1b and Wnt1 in mesencephalon and metencephalon development. *Development* **129**, 5269-77.
- Maves, L., Jackman, W. and Kimmel, C. B.** (2002). FGF3 and FGF8 mediate a rhombomere 4 signaling activity in the zebrafish hindbrain. *Development* **129**, 3825-37.
- Meek, A.** (1909). The encephalomes and cranial nerves of an embryo of *Acanthias vulgaris*. *Anat. Anz.* **31**, 408-415.
- Mellitzer, G.** (1999). Eph receptors and ephrins restrict cell intermingling and communication. *Nature* **400**, 77-81.
- Meyers, E. N., Lewandoski, M. and Martin, G. R.** (1998). An Fgf8 mutant allelic series generated by Cre- and Flp-mediated recombination. *Nat Genet* **18**, 136-141.
- Millet, S., Bloch-Gallego, E., Simeone, A. and Alvarado-Mallart, R. M.** (1996). The caudal limit of Otx2 gene expression as a marker of the midbrain/hindbrain boundary: a study using in situ hybridisation and chick/quail homotopic grafts. *Development* **122**, 3785-97.
- Millet, S., Campbell, K., Epstein, D. J., Losos, K., Harris, E. and Joyner, A. L.** (1999). A role for *Gbx2* in repression of *Otx2* and positioning the mid/hindbrain organizer. *Nature* **401**, 161-164.
- Miyayama, Y. and Fujimoto, T.** (1977). Fine morphological study of neural tube formation in the teleost, *Oryzias latipes*. *Okajimas Folia Anat Jpn* **54**, 97-120.
- Moens, C. B., Cordes, S. P., Giorgianni, M. W., Barsh, G. S. and Kimmel, C. B.** (1998). Equivalence in the genetic control of hindbrain segmentation in fish and mouse. *Development* **125**, 381-391.
- Moens, C. B. and Prince, V. E.** (2002). Constructing the hindbrain: insights from the zebrafish. *Dev Dyn* **224**, 1-17.
- Molven, A., Njolstad, P. R. and Fjose, A.** (1991). Genomic structure and restricted neural expression of the zebrafish wnt-1 (int-1) gene. *Embo J* **10**, 799-807.

- Mori, H., Miyazaki, Y., Morita, T., Nitta, H. and Mishina, M.** (1994). Different spatio-temporal expressions of three otx homeoprotein transcripts during zebrafish embryogenesis. *Brain Res Mol Brain Res* **27**, 221-31.
- Neal, H. V.** (1898). The segmentation of the nervous system in *Squalus acanthias*. *Bull. Mus. comp. Zool. Harv.* **293-315**.
- Nieto, M. A., Gilardi-Hebenstreit, P., Charnay, P. and Wilkinson, D. G.** (1992). A receptor protein tyrosine kinase implicated in the segmental patterning of the hindbrain and mesoderm. *Development* **116**, 1137-50.
- Nieuwkoop, P. D., Nigtevecht, G. V.** (1954). Neural activation and transformation in explants of competent ectoderm under the influence of fragments of anterior notochord in Urodeles. *J. Embryol. Exp. Morph.* **2**, 175-193.
- Niss, K. and Leutz, A.** (1998). Expression of the homeobox gene GBX2 during chicken development. *Mech Dev* **76**, 151-5.
- Nüsslein-Volhard, C. and Wieschaus, E.** (1980). Mutations affecting segment number and polarity in *Drosophila*. *Nature* **287**, 795-801.
- O'Rourke, N. A., Dailey, M. E., Smith, S. J. and McConnell, S. K.** (1992). Diverse migratory pathways in the developing cerebral cortex. *Science* **258**, 299-302.
- O'Rourke, N. A., Sullivan, D. P., Kaznowski, C. E., Jacobs, A. A. and McConnell, S. K.** (1995). Tangential migration of neurons in the developing cerebral cortex. *Development* **121**, 2165-76.
- Oppenheimer, J. M.** (1936). The development of isolated blastoderms of *Fundulus heteroclitus*. *J exp Zool* **72**, 247-279.
- Orr, H.** (1887). Contribution to the embryology of the lizard. *J. Morph.* **1**, 311-372.
- Packard, D. S., Jr., Cox, C. and Poole, T. J.** (2000). Improved techniques for avian embryo culture, somite cell culture, and microsurgery. *Methods Mol Biol* **137**, 185-99.
- Palmgren, A.** (1921). Embryological and morphological studies on the midbrain and cerebellum of vertebrates. *Acta Zool. (Stockholm)* **2**, 1-94.
- Papan, C., Campos-Ortega, J.A.** (1994). On the formation of the neural keel and neural tube in the zebrafish *Danio (Brachydanio) rerio*. *Roux's Archives in Developmental Biology* **203**, 178-186.
- Pauls, S., Geldmacher-Voss, B. and Campos-Ortega, J. A.** (2001). A zebrafish histone variant H2A.F/Z and a transgenic H2A.F/Z:GFP fusion protein for in vivo studies of embryonic development. *Dev Genes Evol* **211**, 603-10.
- Peppelenbosch, M. P., Tertoolen, L. G., de-Laat, S. W. and Zivkovic, D.** (1995). Ionic responses to epidermal growth factor in zebrafish cells. *Exp Cell Res* **218**, 183-8.
- Pfeffer, P. L., Gerster, T., Lun, K., Brand, M. and Busslinger, M.** (1998). Characterization of three novel members of the zebrafish *Pax2/5/8* family:

- dependency of *Pax5* and *Pax8* expression on the *Pax2.1(noi)* function. *Development* **125**, 3063-3074.
- Puelles, L., Marín, F., Martínez-de-la-Torre, M. and Martínez, S.** (1996). The midbrain-hindbrain junction: a model system for brain regionalization through morphogenetic neuroepithelial interactions. In *Mammalian Development*, (ed. P.Lonai), pp. 173-197: Harwood.
- Raible, F. a. B., M.** (2004). Divide et impera- the midbrain-hindbrain boundary and its organizer. *Trends Neurosci in press*.
- Reichenbach, A., Schaaf, P. and Schneider, H.** (1990). Primary neurulation in teleosts--evidence for epithelial genesis of central nervous tissue as in other vertebrates. *J Hirnforsch* **31**, 153-8.
- Reifers, F., Böhli, H., Walsh, E. C., Crossley, P. H., Stainier, D. Y. R. and Brand, M.** (1998). *Fgf8* is mutated in zebrafish *acerebellar* mutants and is required for maintenance of midbrain-hindbrain boundary development and somitogenesis. *Development* **125**, 2381-2395.
- Rhinn, M. and Brand, M.** (2001). The midbrain--hindbrain boundary organizer. *Curr Opin Neurobiol* **11**, 34-42.
- Rhinn, M., Lun, K., Amores, A., Yan, Y. L., Postlethwait, J. H. and Brand, M.** (2003). Cloning, expression and relationship of zebrafish *gbx1* and *gbx2* genes to Fgf signaling. *Mech Dev* **120**, 919-36.
- Schechtman, A. M.** (1942). The mechanics of amphibian gastrulation I. Gastrulation-producing interactions between various regions of an anuran egg (*Hya regilla*). *Univ Calif Publ Zool* **51**, 1-39.
- Schilling, T. F., Prince, V. and Ingham, P. W.** (2001). Plasticity in zebrafish *hox* expression in the hindbrain and cranial neural crest. *Dev Biol* **231**, 201-16.
- Schmitt, S.** (1999). Morphogenetische Untersuchungen zur Entwicklung der Mittel-Hinterhirn-Organisator Region im Zebrafisch, *Danio rerio*. *Diploma Thesis*.
- Schmitz, B.** (1993). Neurulation in the anterior trunk region of the zebrafish *Brachydanio rerio*. *Developmental Biology* **202**, 250-259.
- Senut, M. C. and Alvarado-Mallart, R. M.** (1986). Development of the retinotectal system in normal quail embryos: cytoarchitectonic development and optic fiber innervation. *Brain Res* **394**, 123-40.
- Shimamura, K. and Rubenstein, J. L.** (1997). Inductive interactions direct early regionalization of the mouse forebrain. *Development* **124**, 2709-2718.
- Simeone, A., Acampora, D., Gulisano, M., Stornaiuolo, A. and Boncinelli, E.** (1992). Nested expression domains of four homeobox genes in developing rostral brain. *Nature* **358**, 687-90.
- Simon, J. Z., Cooper, M. S.** (1995). Calcium Oscillations and Calcium Waves Coordinate Rhythmic Contractile Activity Within the Stellate Cell Layer of Medaka Fish Embryos. *J Exp Zool* **273**, 118-129.
- Small, J., Rottner, K., Hahne, P. and Anderson, K. I.** (1999). Visualising the actin cytoskeleton. *Microsc Res Tech* **47**, 3-17.

- Spemann, H., Mangold, H.** (1924). Über Induktion von Embryonalanlagen durch Implantation artfremder Organisatoren. *Wilhelm Roux Arch. Entw. Mech.* **100**, 599-638.
- Steinberg, M. S.** (1963). Reconstruction of tissues by dissociated cells. Some morphogenetic tissue movements and the sorting out of embryonic cells may have a common explanation. *Science* **141**, 401-8.
- Stern, C. D.** (1999). Grafting of somites. *Methods Mol Biol* **97**, 255-64.
- Stern, C. D.** (2001). Initial patterning of the central nervous system: how many organizers? *Nat Rev Neurosci* **2**, 92-8.
- Strahle, U. and Blader, P.** (1994). Early neurogenesis in the zebrafish embryo. *Faseb J* **8**, 692-8.
- te Kronnie G, S. H., Schipper H, Samallo J.** (2000). Teleost yolk cell function on blastoderm differentiation and morphogenesis. *Neth J Zool* **50**, 37-51.
- Tepass, U., Godt, D. and Winklbauer, R.** (2002). Cell sorting in animal development: signalling and adhesive mechanisms in the formation of tissue boundaries. *Curr Opin Genet Dev* **12**, 572-82.
- Trainor, P. and Krumlauf, R.** (2000). Plasticity in mouse neural crest cells reveals a new patterning role for cranial mesoderm. *Nat Cell Biol* **2**, 96-102.
- Trevarrow, B., Marks, D. L. and Kimmel, C. B.** (1990). Organization of hindbrain segments in the zebrafish embryo. *Neuron* **4**, 669-679.
- Trinkaus, J. P. and Drake, J. W.** (1956). Exogenous control of morphogenesis in isolated *Fundulus* blastoderms by nutrient factors. *J Exp Zool* **132**, 311-347.
- Tung, T. and Chang, C., Tung, Y.** (1945). Experiments of the Developmental Potencies of Blastoderms and Fragments of Teleostean Eggs Separated Latitudinally. *Proc. Zool. Soc. Lond.* **115**, 175-188.
- Tung, T., Tung YFY.** (1944). The development of egg-fragments, isolated blastomeres and fused eggs in the goldfish. *Proc Zool Soc Lond* **144**, 46-64.
- Vaage, S.** (1969). The segmentation of the primitive neural tube in chick embryos (*Gallus domesticus*). *Ergebnisse der Anatomie und Entwicklungsgeschichte* **41**, 3-87.
- Walshe, J., Maroon, H., McGonnell, I. M., Dickson, C. and Mason, I.** (2002). Establishment of hindbrain segmental identity requires signaling by FGF3 and FGF8. *Curr Biol* **12**, 1117-23.
- Waskiewicz, A. J., Rikhof, H. A. and Moens, C. B.** (2002). Eliminating zebrafish pbx proteins reveals a hindbrain ground state. *Dev Cell* **3**, 723-33.
- Wassarman, K. M., Lewandoski, M., Campbell, K., Joyner, A. L., Rubenstein, J. L., Martinez, S. and Martin, G. R.** (1997). Specification of the anterior hindbrain and establishment of a normal mid/hindbrain organizer is dependent on Gbx2 gene function. *Development* **124**, 2923-2934.
- Westerfield, M.** (1994). The zebrafish book. Edition 2.1, Oregon: University of Oregon Press.



- Wilkinson, D. G., Bailes, J. A. and McMahon, A. P.** (1987). Expression of the proto-oncogene int-1 is restricted to specific neural cells in the developing mouse embryo. *Cell* **50**, 79-88.
- Wilson, P. and Keller, R.** (1991). Cell rearrangement during gastrulation of *Xenopus*: direct observation of cultured explants. *Development* **112**, 289-300.
- Wilson, P. A., Oster, G. and Keller, R.** (1989). Cell rearrangement and segmentation in *Xenopus*: direct observation of cultured explants. *Development* **105**, 155-66.
- Wilson, S. I. and Edlund, T.** (2001). Neural induction: toward a unifying mechanism. *Nat Neurosci* **4 Suppl**, 1161-8.
- Wizenmann, A. and Lumsden, A.** (1997). Segregation of rhombomeres by differential chemoaffinity. *Mol Cell Neurosci* **9**, 448-59.
- Woo, K. and Fraser, S. E.** (1995). Order and coherence in the fate map of the zebrafish nervous system. *Development* **121**, 2595-609.
- Wurst, W. and Bally-Cuif, L.** (2001). Neural plate patterning: upstream and downstream of the isthmus organizer. *Nat Rev Neurosci* **2**, 99-108.
- Xu, Q., Holder, N., Patient, R. and Wilson, S. W.** (1994). Spatially regulated expression of three receptor tyrosine kinase genes during gastrulation in the zebrafish. *Development* **120**, 287-99.
- Xu, Q. and Wilkinson, D. G.** (1997). Eph-related receptors and their ligands: mediators of contact dependent cell interactions. *J Mol Med* **75**, 576-86.
- Xu, Q. L.** (1999). In vivo cell sorting in complementary segmental domains mediated by Eph receptors and ephrins. *Nature* **399**, 267-271.
- Zervas, M., Millet, S., Ahn, S. and Joyner, A. L.** (2004). Cell behaviors and genetic lineages of the mesencephalon and rhombomere 1. *Neuron* **43**, 345-57.
- Zimmermann, W.** (1891). Über die Metamerie des Wirbeltierkopfes. *Verh. anat. Ges.* **5**, 107-113.

# Appendix

## Isthmus to midbrain transformation in *ace*

In the publication by Jaszai et al. (Jaszai et al., 2003), we have shown that in the *fgf8* (*acerebellar* – *ace*) mutant, the territory normally fated to become the isthmus constriction is converted to midbrain fate. The main part of the characterization was based on marker analysis in mutant and wild type embryos. To address the behavior of cells located at the same a-p positions in wt and *ace* embryos, I decided to label cells by Dil application, using the technique introduced in the lineage restriction part of my thesis.

I distinguished wt and *ace* embryos at the 5-somite stage based on their morphology: *Ace* embryos have a “bump” of varying size (which is more pronounced at the 10-somite stage, fig. 18 D) at the mhb level of the neural tube, which allowed me to sort them from wt siblings. After labeling, the wound was allowed to heal and the first pictures taken at the age of ten somites (fig. 18 A,D).

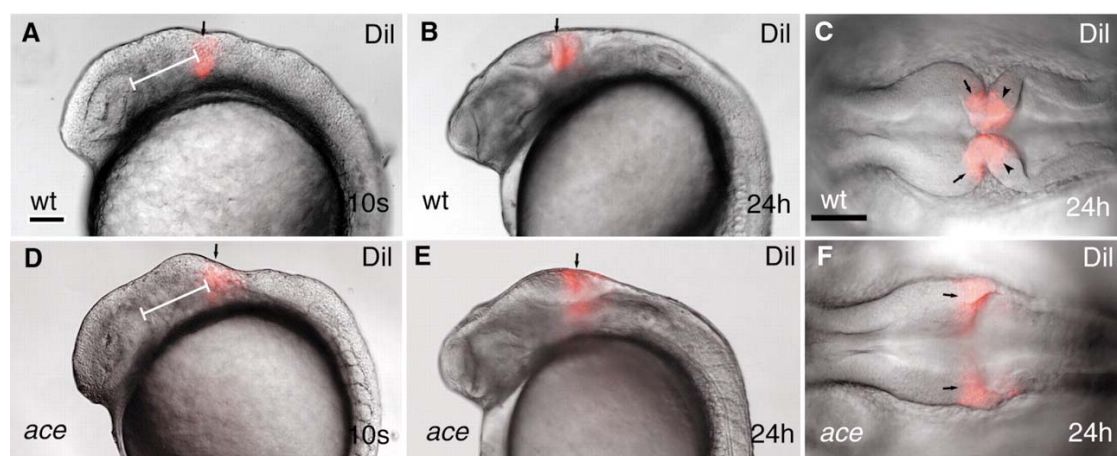


**Figure 18** Dil lineage-tracing reveals fate alteration of mhb cells in *ace* mutants. All views are anterior to the left. (A,B,D,E) Lateral, (C,F) dorsal views. (A-F) Labeling (red) wild-type and *ace* mutant embryos at equivalent a-p positions along the neural axis reveals that the labeled cells in the mutants are not retained in the mhb area. The labeled mutant cells always end up at the caudal enlargement of the tectum (E,F). Arrows (A,B,D,E) point to the Dil-labeled group of cells. Arrows (C,F) point to the mesencephalic side of the labeled area; arrowheads (C) point to the hindbrain side. The white bar (A,F) shows the distance between the caudal edge of the optic vesicle and the Dil label.

To ensure that cells were labeled at equivalent positions along the a-p axis of the embryo, I measured the distance between the posterior end of the optic vesicle and the anterior edge of the Dil label in wt and *ace* embryos (fig. 18, A,D and table 3). In the wt cases analyzed, the labeled cells ended up in the mhb area at 24 hpf (fig. 18 B,C), while in *ace* embryos, the cells were found in the posterior part of the enlarged tectum opticum at this stage (fig. 18, E,F). This argues that cells normally fated to become mhb tissue are transformed into midbrain cells in *fgf8* mutant embryos.

**Table 3** Statistics Dil labeling

	<b>wild type, 7 embryos</b>	<b><i>ace</i>, 8 embryos</b>
Average	155	201
Minimum	134	153
Maximum	182	225
Standard deviation	21	23

The table shows the distance in  $\mu\text{m}$  of the anterior most Dil labeled cells from the posterior tip of the eye field in wt and *ace* embryos at the ten somite stage: In all wild type cases, the labeled cells ended up in either the posterior tectum opticum and/or cerebellum/rhombomere one, i.e. in the mhb region. In all *ace* cases, cells ended up in the posterior part of the enlarged tectum.

It remains a possibility that a specific cell population at the prospective mhb in *ace* embryos dies and therefore accounts at least in part for the loss of cerebellar tissue at later stages. Accumulation of apoptotic cells can be detected in *ace* embryos at mid-somitogenesis stages (Jaszai et al., 2003, fig. 5). As a recent publication in mouse also claims that *Fgf8* is a major survival factor for the developing mhb region (Chi et al., 2003), I suggest that the role of apoptotic cell death in the *ace* phenotype needs further clarification.

## Publications

**Langenberg T.**, Brand M. and Cooper, MS. (2002): Imaging brain development and organogenesis in zebrafish using immobilized embryonic explants. *Developmental Dynamics* 228 (3): 464-74.

Jaszai J., Reifers F., Picker A., **Langenberg T.** and Brand M. (2003): Isthmus-to-midbrain transformation in the absence of midbrain-hindbrain organizer activity. *Development* 130 (26): 6611-23.

A third publication describing the lineage restriction at the mhb is in preparation.

Hiermit versichere ich, dass ich die vorliegende Arbeit ohne unzulässige Hilfe Dritter und ohne Benutzung anderer als der angegebenen Hilfsmittel angefertigt habe; die aus fremden Quellen direkt oder indirekt übernommenen Gedanken sind als solche kenntlich gemacht. Die Arbeit wurde bisher weder im Inland noch im Ausland in gleicher oder ähnlicher Form einer anderen Prüfungsbehörde vorgelegt.

Dresden, den 29.09.04

Dipl.-Biol. Tobias Langenberg